

# Design, Realization, Applications of Gas and Ion Separations Materials



Tina M. Nenoff,\* Jessica M. Rimsza,\*  
Matthew Christian, Matthew Hurlock, Keith J. Fritzsching, D. Jon  
Vogel,  
Susan E. Henkelis, Dorina Sava Gallis

Sandia National Laboratories, Albuquerque, NM USA

**Collaboration:** Co-PIs, Nenoff (Synthesis) & Rimsza (Modeling)

AVS e-talk

Sandia National Laboratories is a multimission laboratory managed and operated by National Technology and Engineering Solutions, LLC., a wholly owned subsidiary of Honeywell International, Inc., for the U.S. Department of Energy's National Nuclear Security Administration under contract DE-NA-0003525.

November 16, 2022

# Outline

- Background

I. RE-DOBDC MOFs for Humid NO<sub>x</sub> acid gas separations  
experiment  
modeling (DFT, AIMD)

II. RE-DOBDC, Entire Lanthanide Series  
reaction parameters  
stages of crystallinity  
kinetic driven denticity

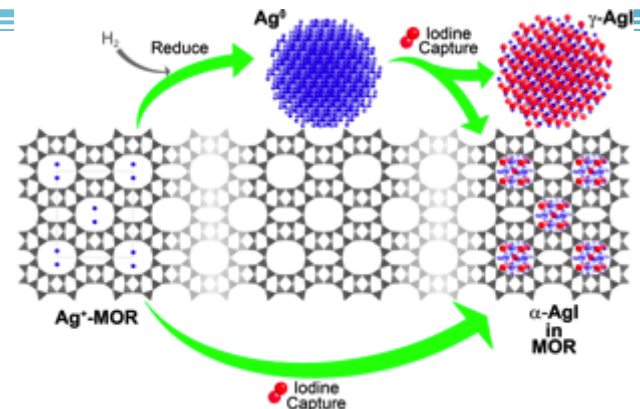
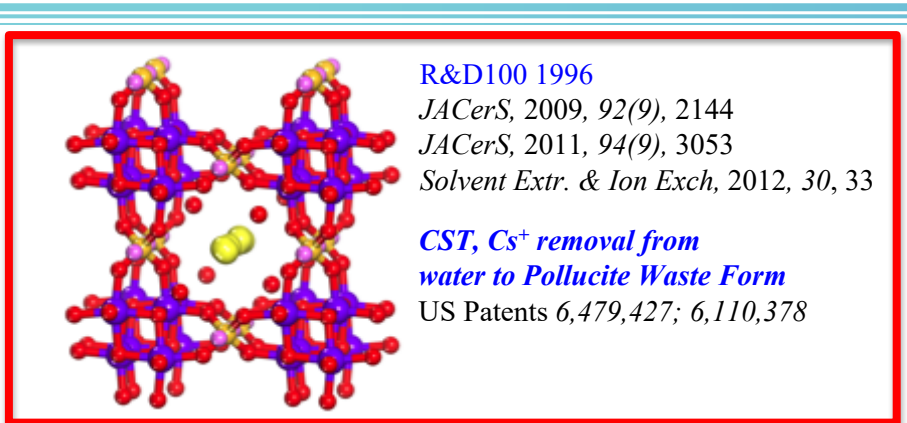
III. Fluorination of the Metal Cluster

IV. Transitioning fundamental DOBDC MOFs to Sensors (applications)

- Conclusion

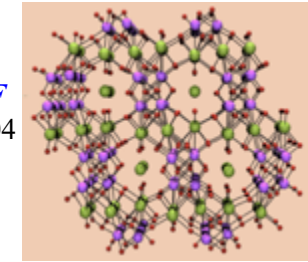
- Info about Sandia, Postdoc & Fellowship positions

# Background: Nanoscale Materials for bulk scale applications

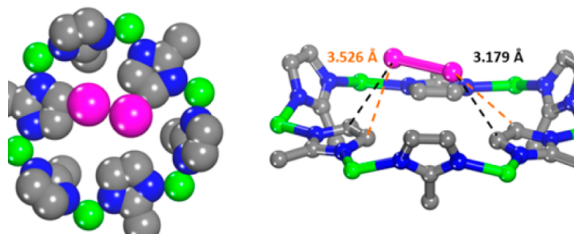


**Ag-MOR**  
***I<sub>2</sub>(g)* capture & mechanisms**

*JACS*, 2010, 132(26), 8897  
*J Phys Chem Lett*, 2011, 2,2742  
*I&ECR* 2017, 56(8), 2331



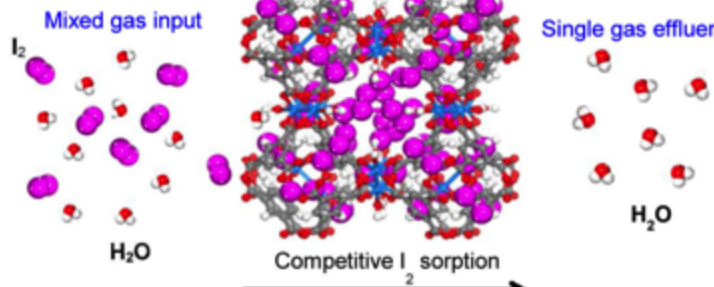
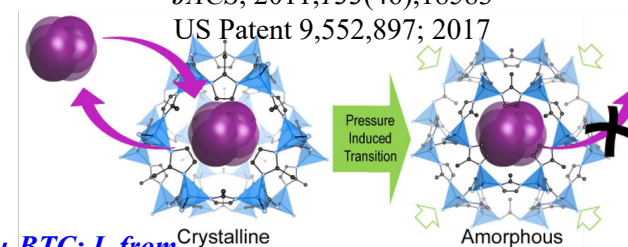
**SOMS, Sr<sup>2+</sup> getter, 1-step to Perovksite WF**  
*JACS*, 2002, 124(3), 1704  
US Patent 7,122,164



**Design on the nanoscale of the Separation Material to optimize on the bulk scale**

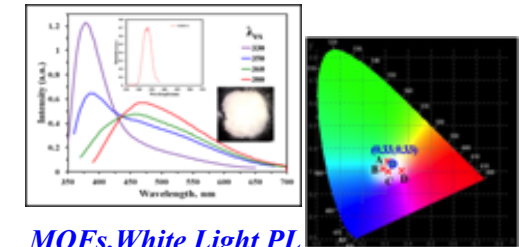
**MOF Amorphization for Gas Storage**

*JACS*, 2011, 133(46), 18583  
US Patent 9,552,897; 2017

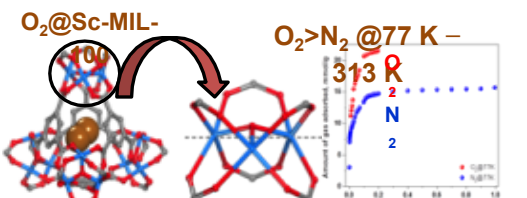
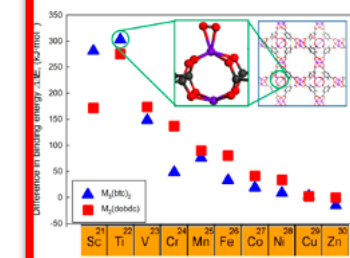


**O<sub>2</sub> Separations with MOFs for Energy Efficient Oxyfuel Combustion**

*Chem. Mater.* 2016, 28(10), 3327-3336  
*Chemical Science* 2016, 18, 11528  
*J. Phys. Chem. C*, 2015, 119, 6556  
*Chem. Mater.* 2015, 27(6), 2018



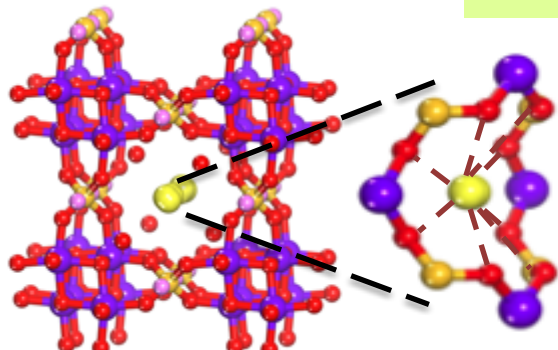
**MOFs, White Light PL**  
*JACS*, 2012, 134(9), 3983  
*Chem Mater*, 2014, 26 (9), 2943



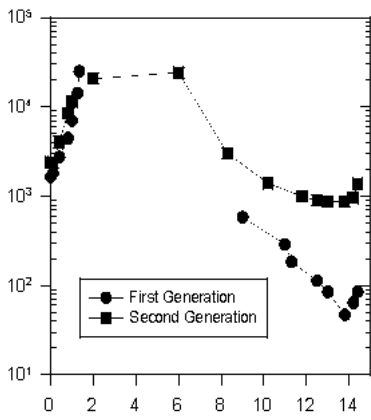
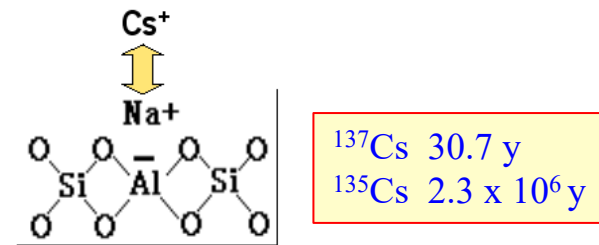
# Early Career, Geo-Inspired: CSTs for Rad Ion High Selectivity and Capture (TRL 1-9)



## CSTs: Crystalline Silico-titanates



Research (1993): Sandia LDRD project – gram reactors  
Development: DOE/EM – 1-5 gallon reactors  
Commercialization: CRADA with UOP Corp.,  
**IONSIV™ IE-910 & IE-911 (Dec 1995)**  
1800 lb lots produced



Sandia: Distribution  
Coefficient of Cs on CST



UOP IONSIV™ IE-911

## Fukushima Daiichi Nuclear Power Plant Accident, March 2011

- 2011 SNL re-licensed CST IP to Honeywell UOP LLC who coordinated with Toshiba for implementation in the SARRY™ Process at Fukushima

**SARRY™: Simplified Active Water Retrieve and Recovery System**  
augmentation of Accumulated Water processing Facility



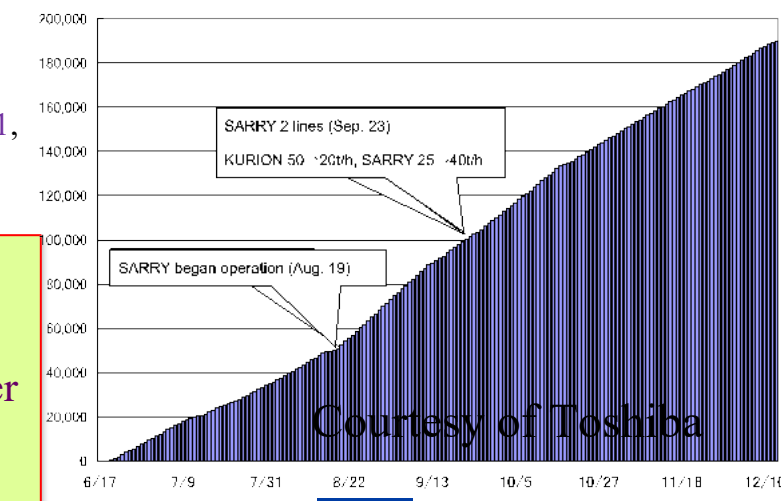
2011: UOP re-licensed CST IP, in production of 40K+ lots within 2 months of Fukushima accident

SARRY was installed August 2011,  
decontamination factors of Cs  
SARRY process is  $5 \times 10^5$

By December 2015,  
160+ million gallons of  
Cs<sup>+</sup> contaminated seawater  
were cleaned with the  
**SARRY™ Process.**  
**Decon work completed.**

Amount of processed water (cumulative) (tons)

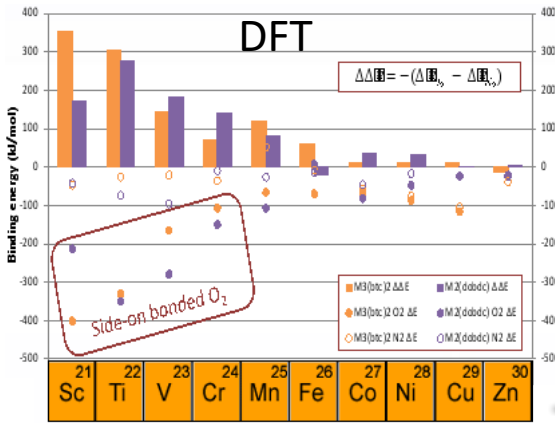
Amount of processed accumulated water



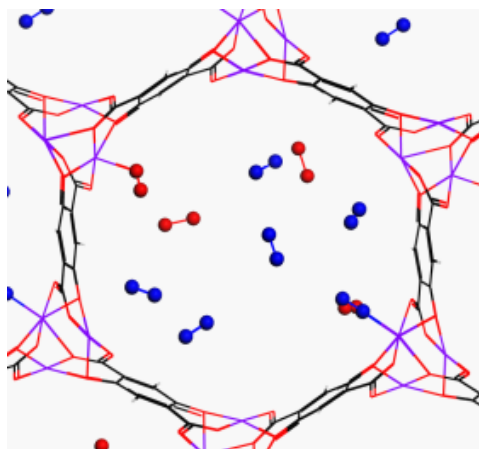
Courtesy of Toshiba

# Midcareer, Computationally Designed: MOF for Ambient O<sub>2</sub> Separations from Air. (TRL 1-7...)

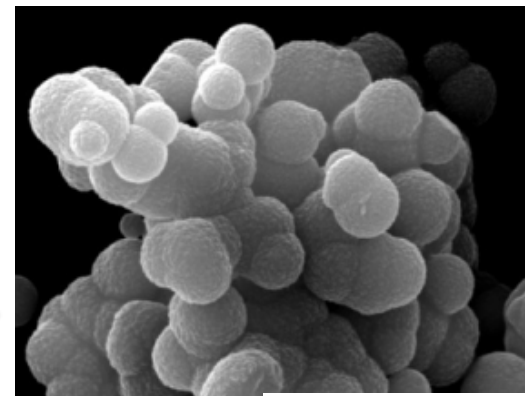
## Computationally Designed Materials



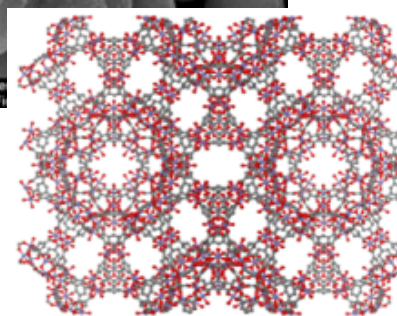
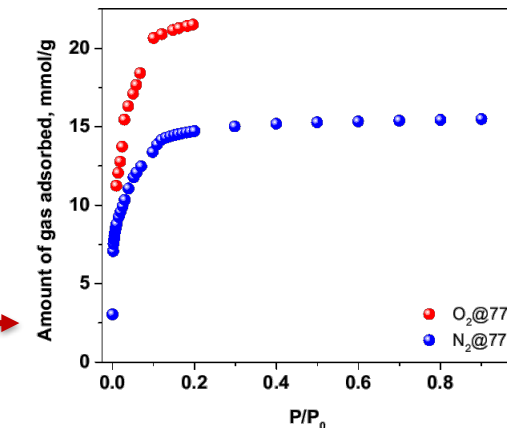
## Ab initio MD



## Novel Materials Synthesis



## Exp Gas Testing



Chem. Mater. 2016, 28(10), 3327  
Chem. Mater. 2015, 27(6), 2018

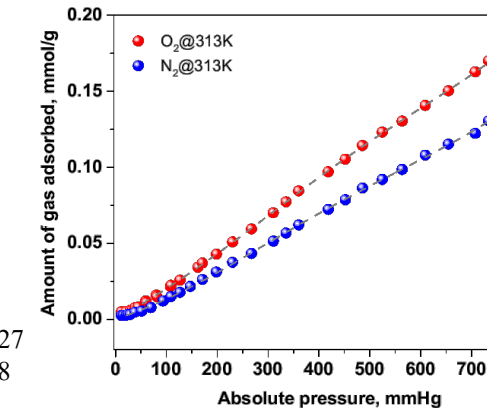
## Industrial Scale Up To Commercialization

IP: US Patent #  
10,549,261  
Awarded Feb 4, 2020

DOE/SBIR Phase I  
FY19 (IP licensed),  
two industrial partners

DOE/SBIR Phase II  
FY21 (IP re-licensed),  
1+ industrial partners

DOE/SBIR Phase II A  
FY22- (IP re-licensed),  
1+ industrial partners



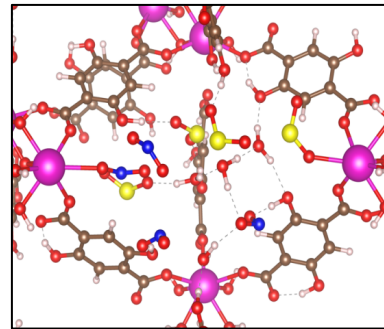
# Computationally Driven, Experimentally Validated, Rapid Materials Discovery. BES/EFRC: UNCAGE-ME\*



\*Center for Understanding and Control of Acid Gas-Induced Evolution of Materials for Energy

## TRL 1: Design and tune adsorbents to selectively adsorb industrial caustic acid gases

Optimized Eu-DOBDC + 4H<sub>2</sub>O + 4NO<sub>2</sub> + 4SO<sub>2</sub>



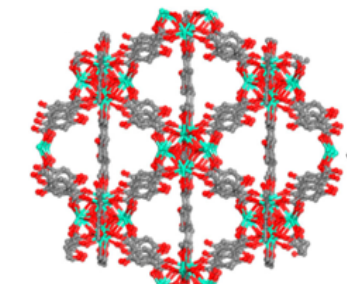
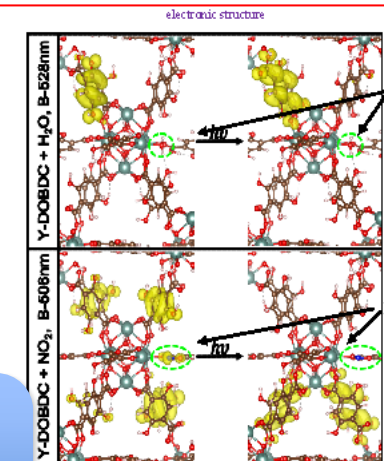
DFT & AIMD for mixed Gas competitive binding  
PCCP, 2019, 21, 23085  
ACS AMI, 2020, 12, 4, 4531  
Angew Chemie, 2021, 60(20), 11514

Computation

Mixed gas adsorption  
Testing

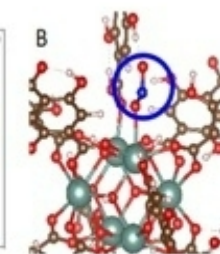
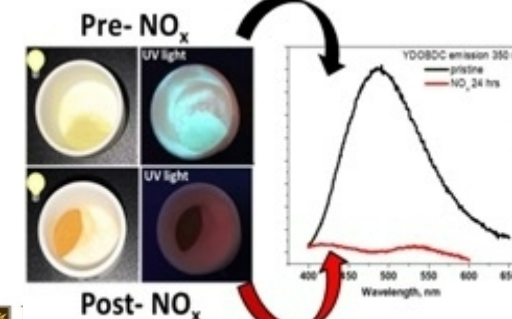
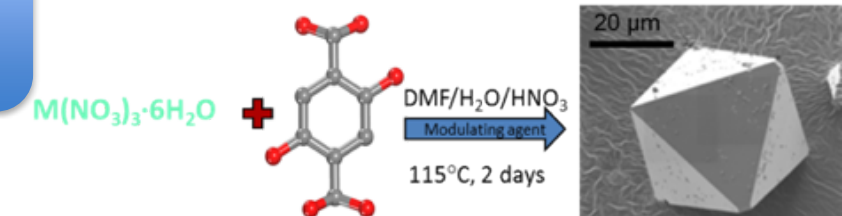
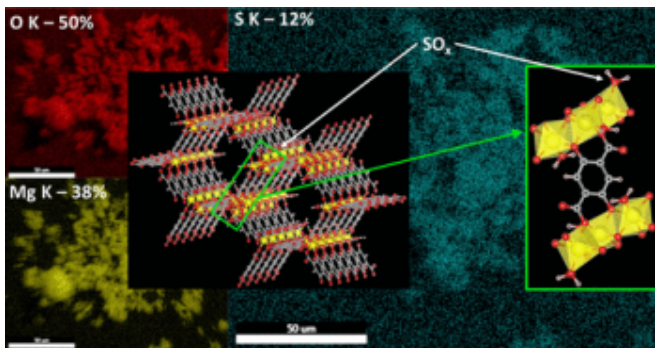
Materials  
Synthesis

Characterization



Industrial Acid Gas Adsorbents:  
RE-DOBDC MOFs  
ACS AMI 2019, 11, 46, 43270  
ACS AMI, 2020, 12, 17, 19504  
ACS AMI, 2020 12, 20, 22845  
ACS AMI, 2021, submitted

Mixed H<sub>2</sub>O + SO<sub>x</sub> adsorption testing  
ACS AMI, 2021, 13, 7278

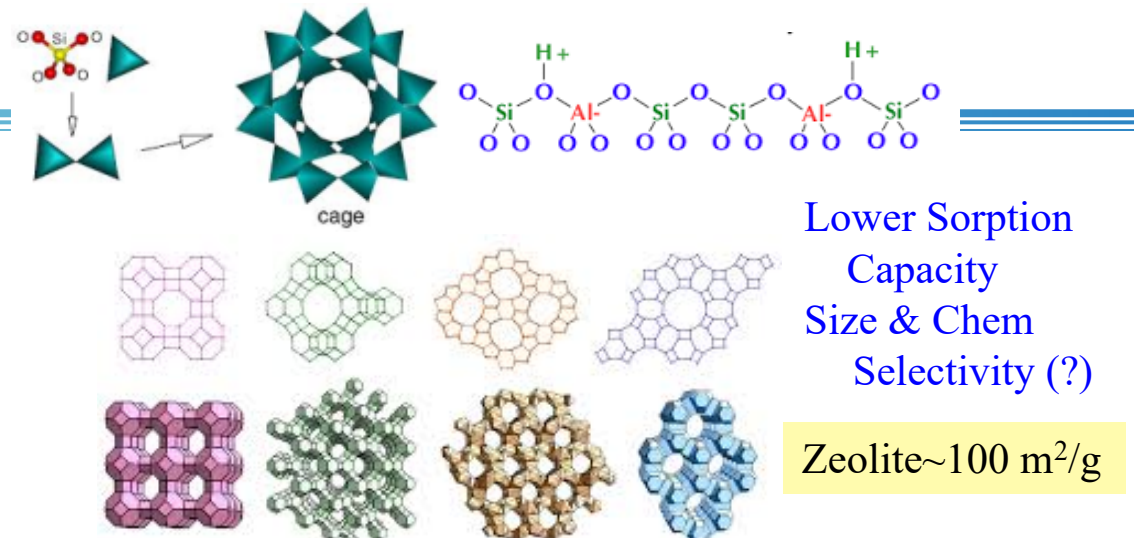


# Nanoporous Gas Adsorption Materials

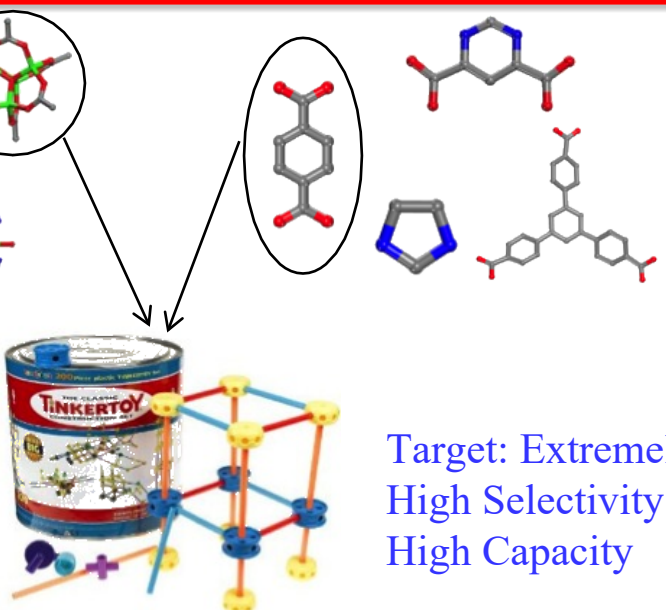


Activated Carbon/  
Charcoal  $> 500 \text{ m}^2/\text{g}$

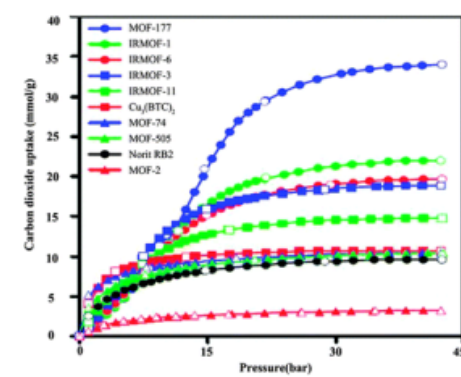
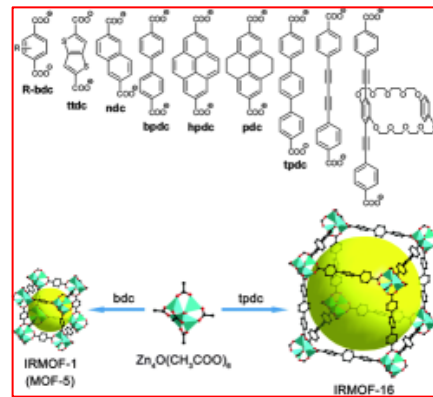
Higher sorption capacity  
Lower Selectivity  
Saturation from background gases



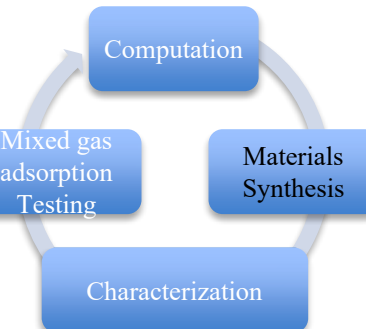
Metal-Organic Frameworks (MOFs)  $> 1000 \text{ m}^2/\text{g}$



Target: Extremely High Selectivity & High Capacity



# I. Rare Earth – DOBDC MOFs, Acid Gas Durability



How to design and tune adsorbents to selectively adsorb acid gases?

**Rare earth elements have been shown to preferentially bind to acid gases:**  
**Optimization of binding to framework but not too strong as to be destructive**

- Lanthanide oxygen-sulfur catalysts (Kay et.al, US Patent 5,213,779 (1993))
- Metal organic coordination polymers with  $Tb^{3+}$  have a strong affinity and coordination binding to  $H_2S$  (Anal. Chem, 2013, 85,22,11020)
- Europium has high selectivity for hydrogen sulfide (Dalton Trans., 2016, 45, 928)

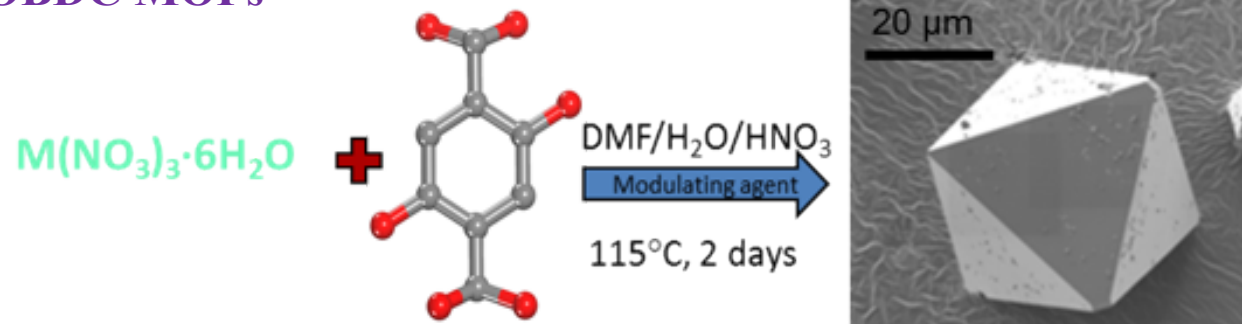


Dorina Sava Gallis



Susan Henkelis

## RE-DOBDC MOFs



Unit Cell =  $RE_{12}(\mu_3-OH)_{16}(C_8O_6H_4)_8(C_8O_6H_5)_4 + 12 H_2O$   
**M = RE = Y, Eu, Tb, Yb**  
DOBDC = 2,5-dioxido-1,4-benzenedicarboxylate

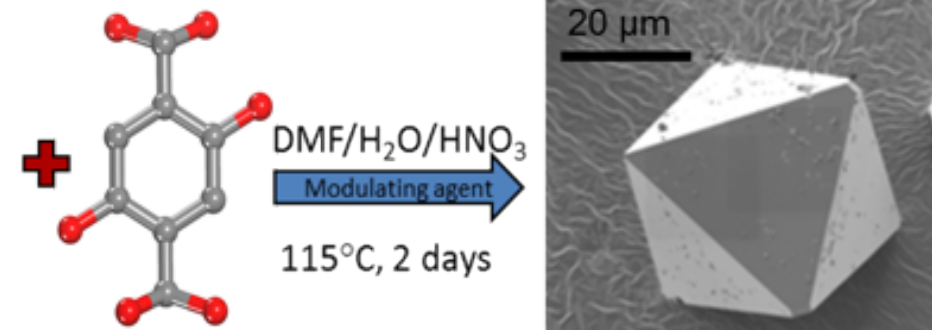
Sava Gallis *et al.* *ACS Appl. Mater. Interfaces* 2017, 9, 22268; *CrystEngComm* 2018, 20, 5919; *JPPC* 2018, 122, 47, 26889

# RE-DOBDC MOFs

RE = M = Y, Eu, Tb, Yb

DOBDC = 2,5-dioxido-1,4-benzenedicarboxylate

$M(NO_3)_3 \cdot 6H_2O$



Single-crystal X-ray diffraction

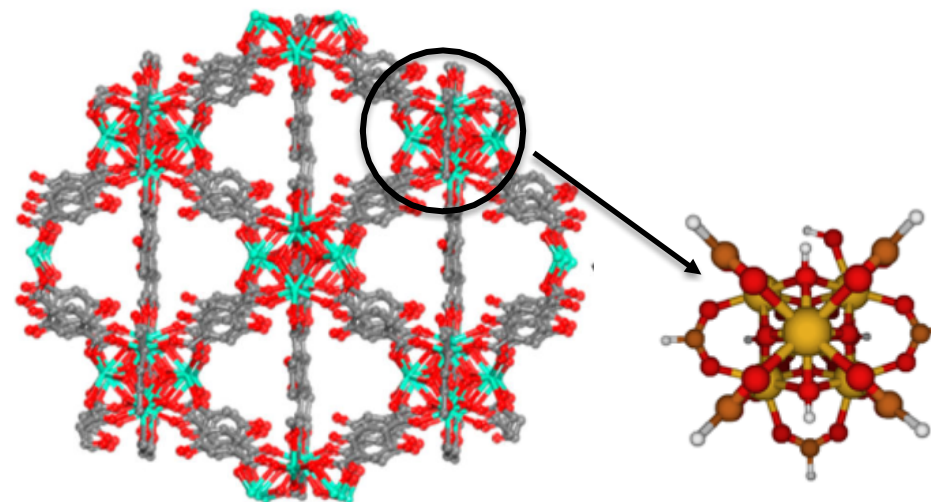
Eu-DOBDC

Tetragonal, 3D framework  $P4nc$

$a = b = 15.5567 \text{ \AA}$

$c = 21.334 \text{ \AA}$

$\alpha = \beta = \gamma = 90^\circ = V = 5163.06 \text{ \AA}^3$



Unit Cell =

$RE_{12}(\mu_3-OH)_{16}(C_8O_6H_4)_8(C_8O_6H_5)_4 + 12 H_2O$

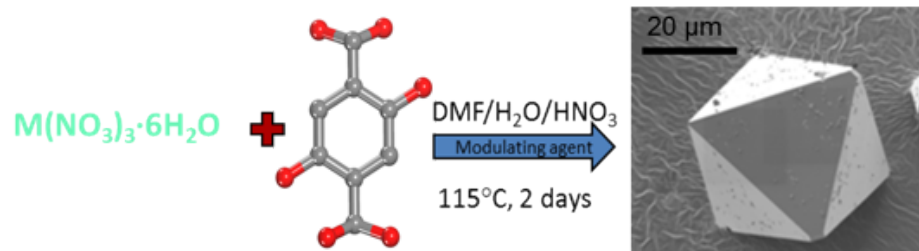
The RE-DOBDC platform is based on building block akin to prototypical Zr-hexanuclear cluster of UiO-66 yet with an unsaturated metal bond.

A combination of monodentate and bidentate linker bonding to metal center

Resultant **RE-DOBDC MOFs**

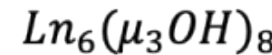
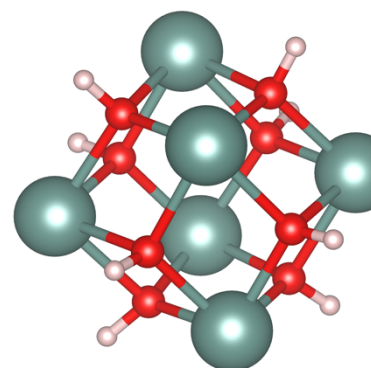
Octahedral cages of  $\sim 14 \text{ \AA}$  diameter, accessible via triangular windows of  $\sim 5.5 \text{ \AA}$

# RE-DOBDC MOFs

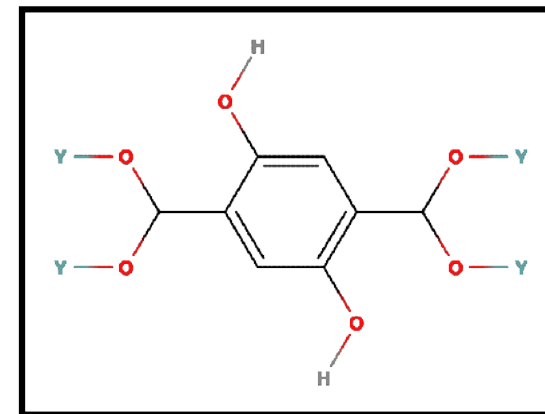


- Lanthanides provide unique characteristics not found in transition metals.
- High coordination numbers (8-9) and new optical transitions facilitated by 4f electrons.

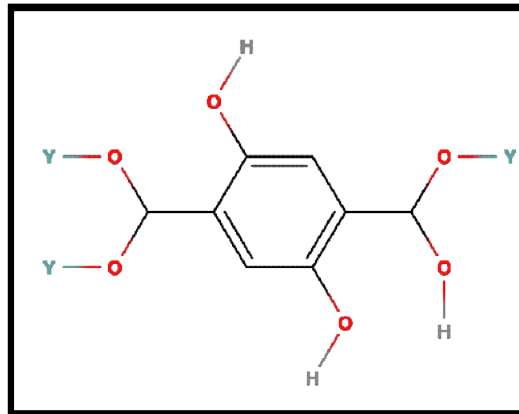
Metal Centers



DOBDC Organic Linkers  
Bidentate



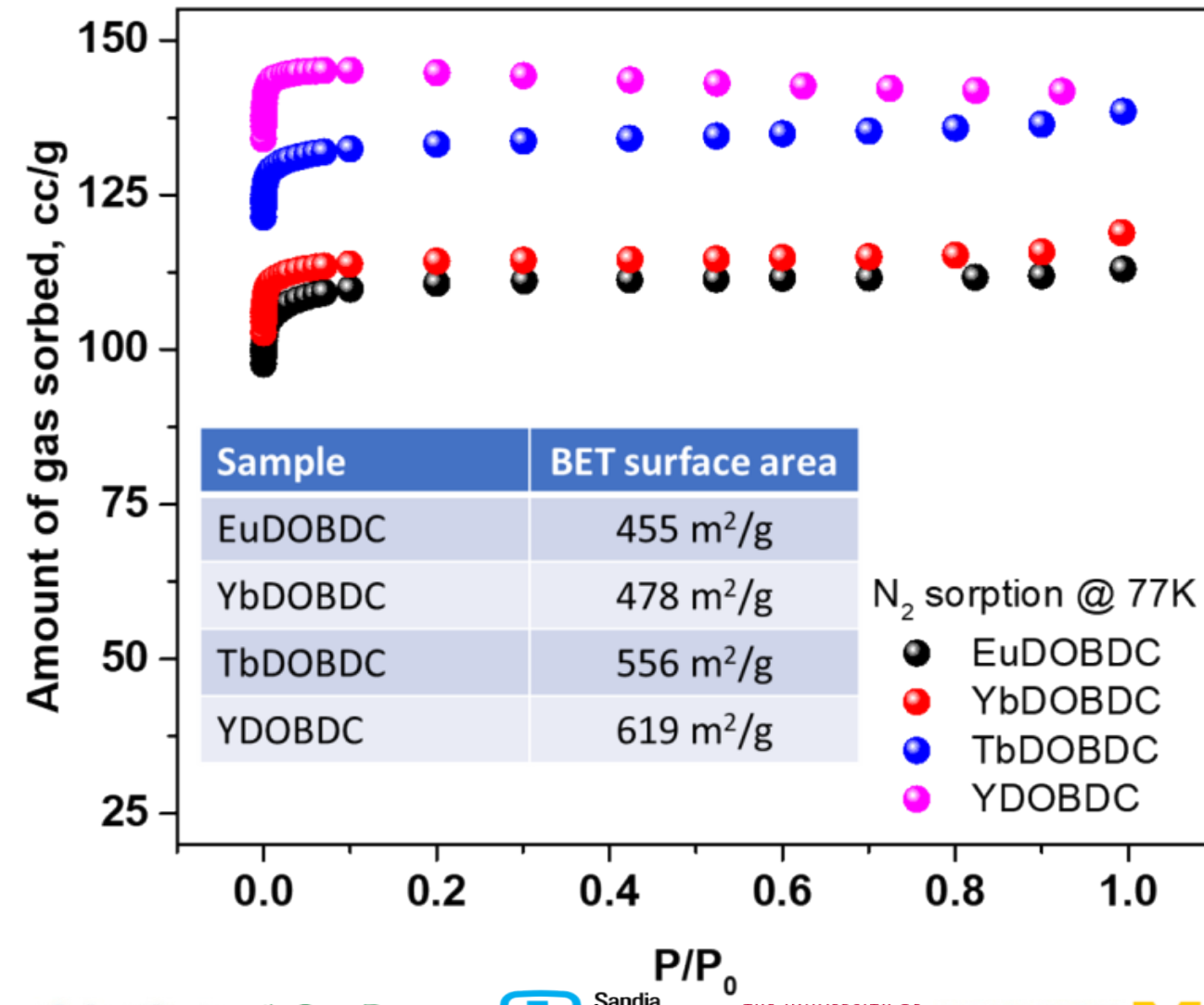
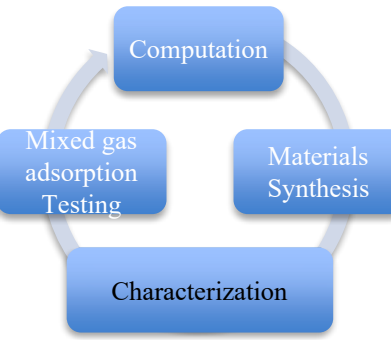
Monodentate



39	Y	57	La	58	Ce	59	Pr	60	Nd	61	Pm	62	Sm	63	Eu	64	Gd	65	Tb	66	Dy	67	Ho	68	Er	69	Tm	70	Yb	71	Lu
	Yttrium 88.906		Lanthanum 138.905		Cerium 140.116		Praseodymium 140.908		Neodymium 144.243		Promethium 144.913		Samarium 150.36		Europium 151.964		Gadolinium 157.25		Terbium 158.925		Dysprosium 162.500		Holmium 164.930		Erbium 167.259		Thulium 168.934		Ytterbium 173.055		Lutetium 174.967

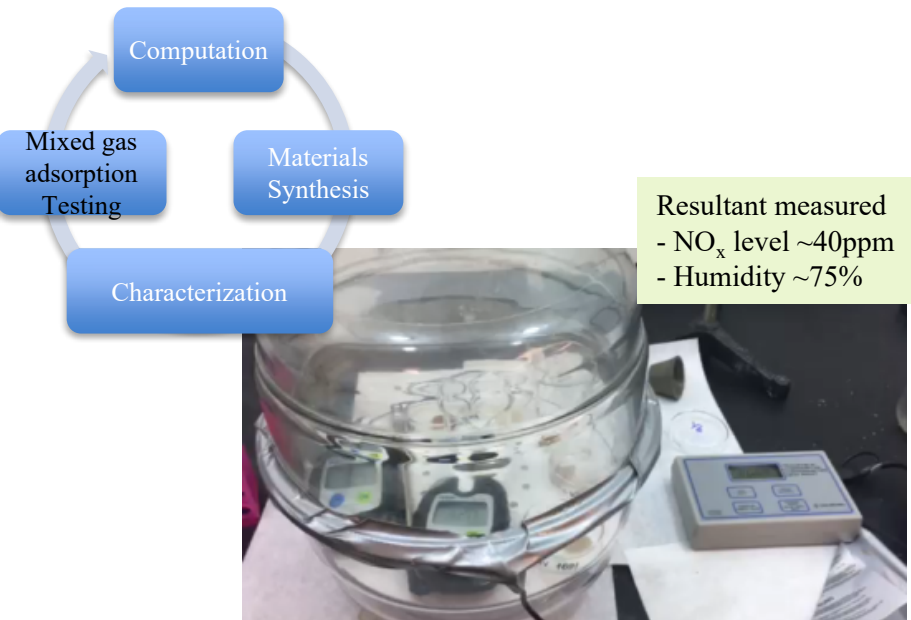
Vogel, D. J., et. al., *PCCP* **2019**, 21, 23085-23093. Sava Gallis, D. F., et. al., *ACS Appl. Mater. Interfaces* **2019**; Sava Gallis *et al.* *ACS Appl. Mater. Interfaces* **2017**, 9, 22268; *CrystEngComm* **2018**, 20, 5919; *JPPC* **2018**, 122, 47, 26889

# BET adsorption data confirming open porosity



# Mixed Gas: $\text{H}_2\text{O} + \text{NO}_x$ adsorption, RE-DOBDC MOFs (RE = Y, Yb, Tb, Eu)

Sava Gallis, Vogel, D. J.; Vincent, G.; Rimsza, J. M.; Nenoff, T.M., *ACS Appl. Mater. Interfaces* 2019, 11(46), 43270

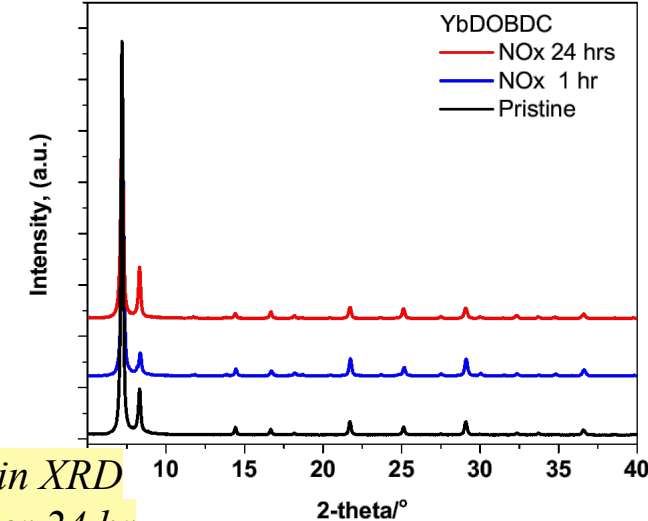
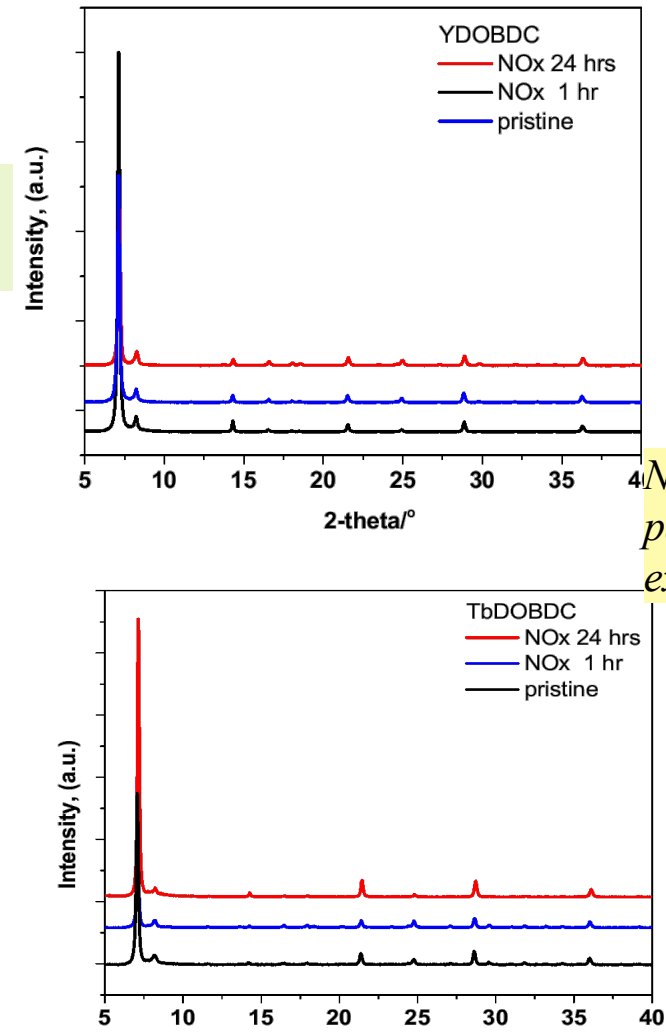


$\text{NO}_x$  is generated in an adsorption chamber at room temperature

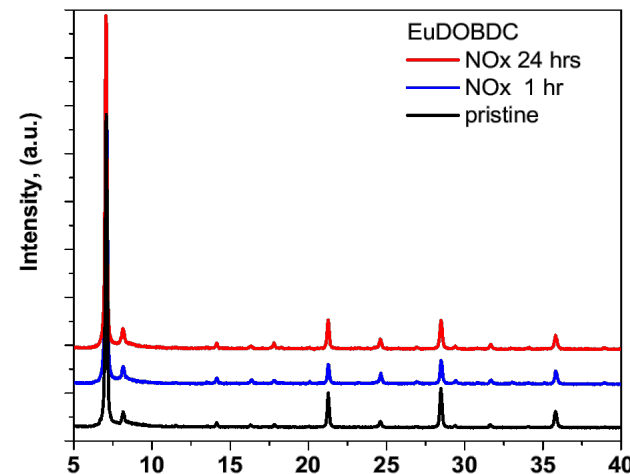
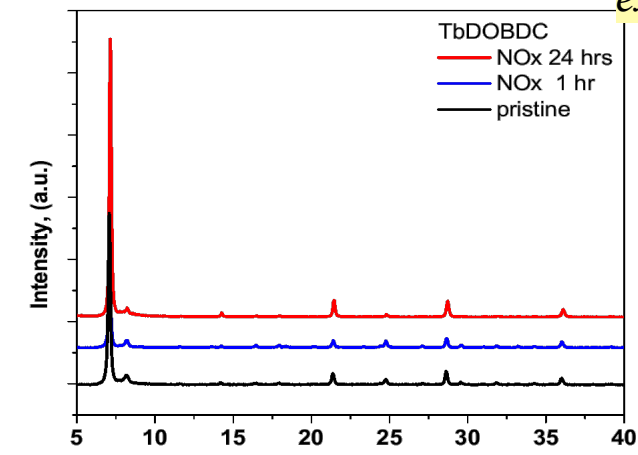
**1<sup>st</sup> step:** Generation of nitrous acid via acidification with  $\text{H}_2\text{SO}_4$   
 $2 \text{NaNO}_2 + \text{H}_2\text{SO}_4 \rightarrow 2 \text{HNO}_2 + \text{Na}_2\text{SO}_4$   
**2<sup>nd</sup> step:** Nitrous acid decomposition  
 $2 \text{HNO}_2 \rightarrow \text{NO}_2 + \text{NO} + \text{H}_2\text{O}$

## Bulk $\text{NO}_x$ prep from UNCAGE-ME team:

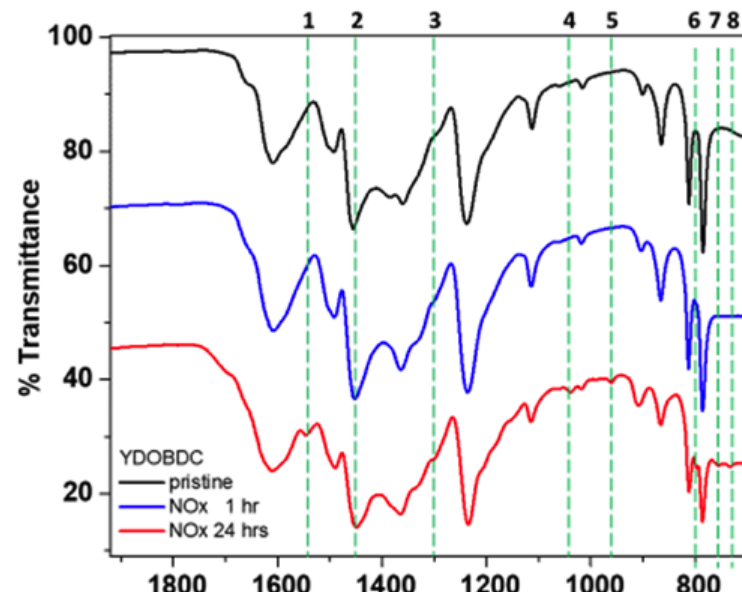
Bhattacharyya, Han, Joshi, Zhu, Lively, Walton, Sholl, Nair  
*J. Phys. Chem. C.* 2019, 123, 2336



No change in XRD patterns after 24 hr exposure



# Y-DOBDC: IR and thermal data showing nanopore adsorption of NO<sub>x</sub> species

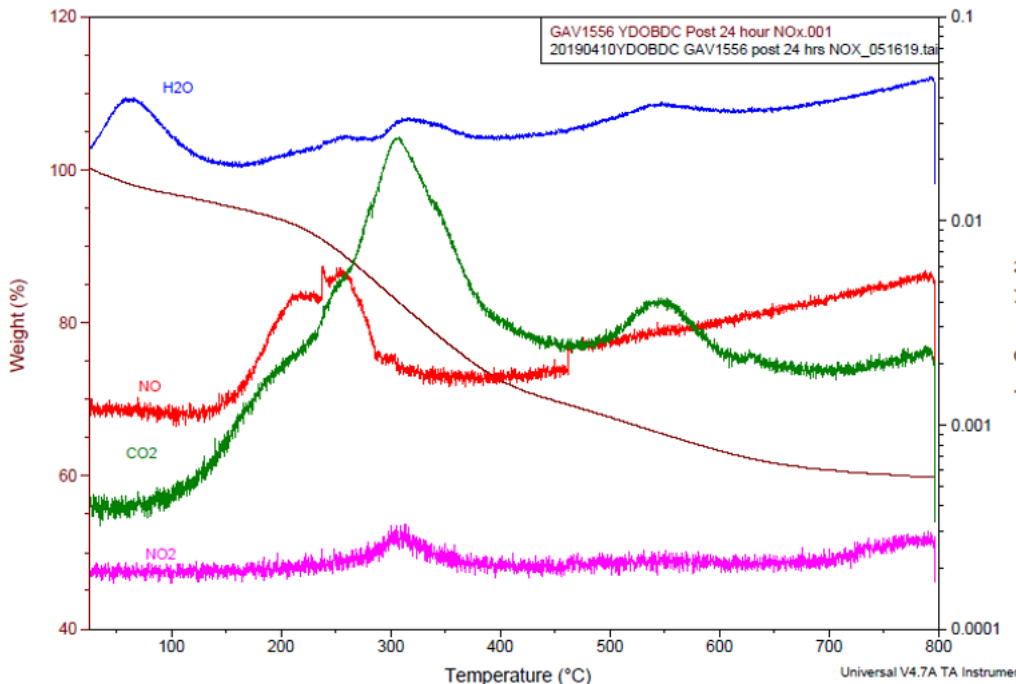


Peak number	Wavenumber (cm <sup>-1</sup> )	Peak assignment
1	1544	Asym. NO <sub>2</sub> stretch
2	1325	Sym. NO <sub>2</sub> stretch
3	1296	Asymmetric NO <sub>2</sub> stretch (R-ONO <sub>2</sub> )
4	1206	C-O stretches of organic nitrates/nitrite
5	1177	C-O stretches of organic nitrates/nitrite
6	1038	symmetric NO <sub>2</sub> stretch (R-ONO <sub>2</sub> )
7	960	aromatic C-N stretch of the nitro group
8	797	N-O stretch (R-ONO)
9	755	NO <sub>2</sub> deformation in R-ONO <sub>2</sub> ; N-O stretch in R-ONO
10	733	NO <sub>2</sub> deformation in R-ONO <sub>2</sub>

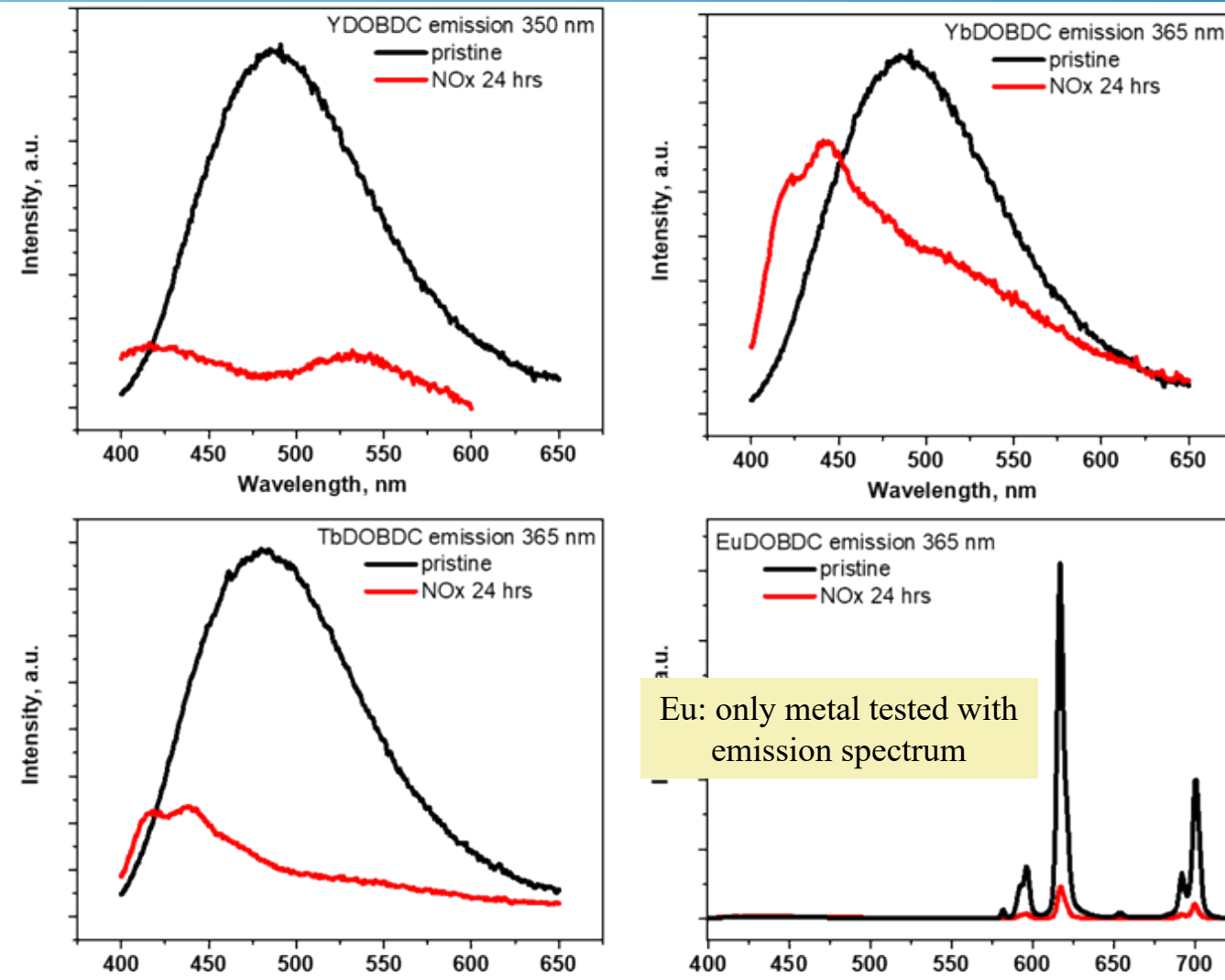
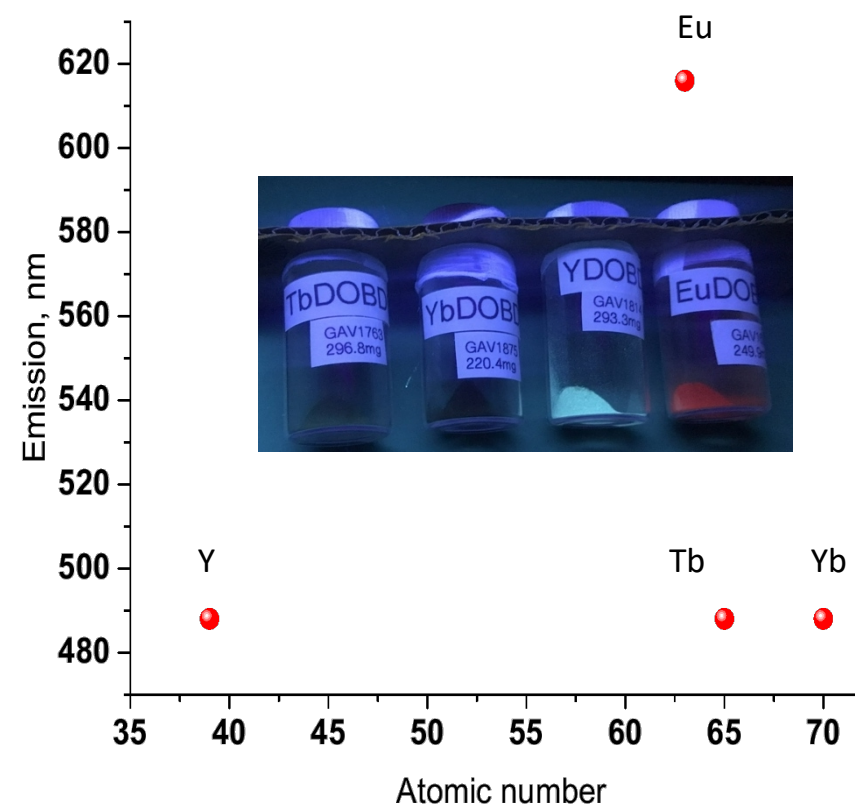
Peak assessments from  
- *Chem. Mater.* **2017**, *29*, 4227  
- Bhattacharyya, Han, Joshi, Zhu, Lively, Walton, Sholl, Nair  
*J. Phys. Chem. C* **2019**, *123*, 2336

2NO<sub>2</sub> → 2NO + O<sub>2</sub> @ 150°C in all plots,  
confidence between IR and TGA that NO<sub>2</sub> adsorbed

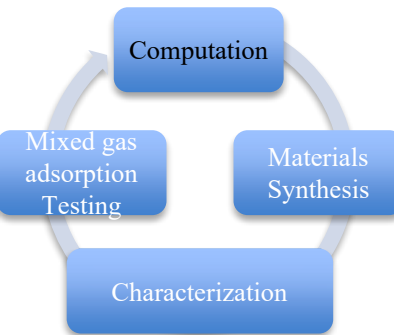
Representative IR and TGA/MS of all analogs in series



# Emission data per unique metal centers, Quenching with $\text{NO}_x$ adsorption



# Computational Approach: Modeling f-electron containing systems



How to efficiently simulate RE-MOFs and accurately calculate (i) the geometric and (ii) the electronic structure?

## Different Methods/Corrections Tested:

- **Large core potential (LCP):** 4f-electrons in Ln is treated as part of the core (limited involvement in bonding and adsorption properties)
- **Full valence potential:** simulated 4f-electrons as valence (can be involved in bonding and adsorption)
- **Hubbard corrections (1-9):** used to correctly simulate band gap energies with f-electron containing molecules
- **Spin restricted/unrestricted:** changes if electrons must be pair (restricted) or unpaired (unrestricted)



### Additional Details:

Vienna *ab initio* Simulation Package  
 PBEsol exchange correlation functional  
 DFT-D3 used for vdW interactions  
 Gamma point calculation

### Validation of calculated binding energies

UNCAGE-ME Collaborative Studies, Univ AL, Dixon Group:  
 Performing higher order (e.g. coupled cluster)  
 calculations on smaller clusters of the MOF structure,  
 Binding with different gas molecules,  
 Validation of calculated binding energies

Vogel, D.J.; Sava Gallis, D.F.; Nenoff, T.M.; Rimsza, J.M.  
*PCCP*, 2019, 21, 23085-23093.

Dixon, et. al., *Comput. Theor. Chem.*, 2017, 1120, 46



Jessica Rimsza



D. Jon Vogel

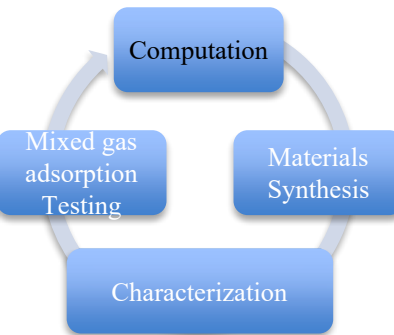
# Use of DFT modeling to explain structure – property relationships of RE-DOBDC MOF



D. Jon Vogel

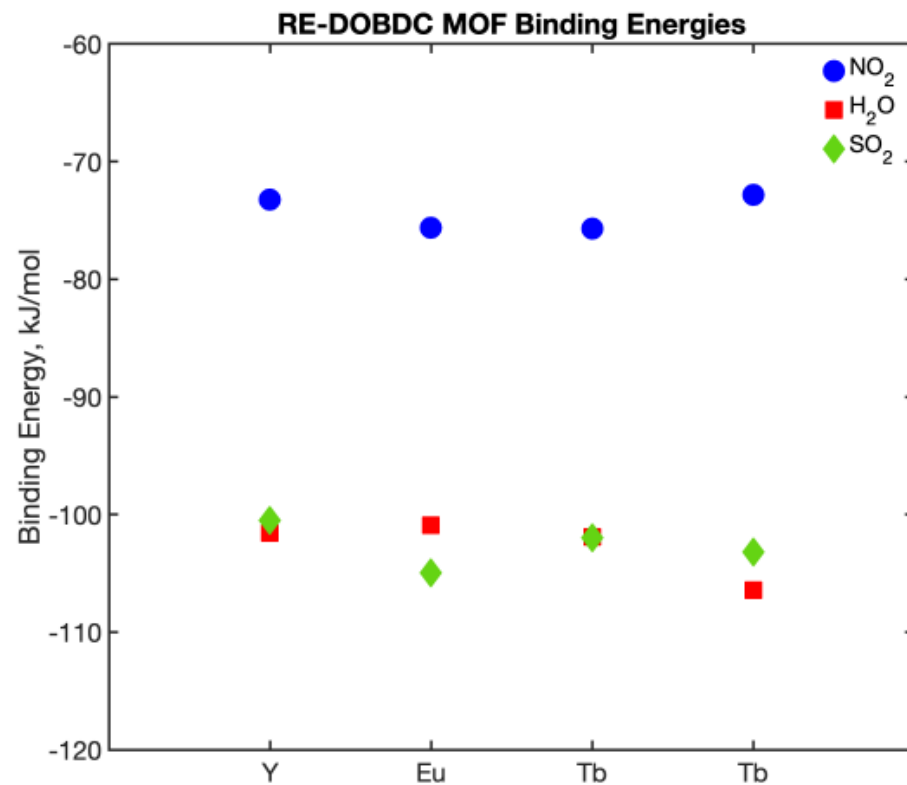


Jessica Rimsza



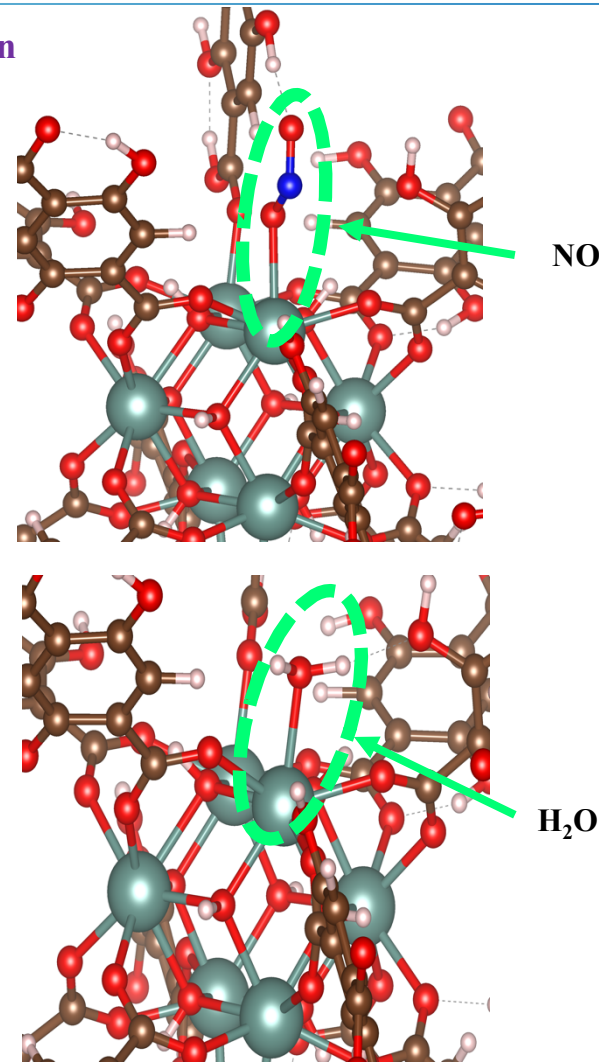
## Experimental data is supported and explained by complimentary DFT modelin

- Experimental MOFs PXRD: all stable under 24hr humid  $\text{NO}_x$  exposure
- Calculated binding energies for  $\text{H}_2\text{O}$  &  $\text{NO}_2$ : unsaturated metal sites prefer  $\text{H}_2\text{O}$



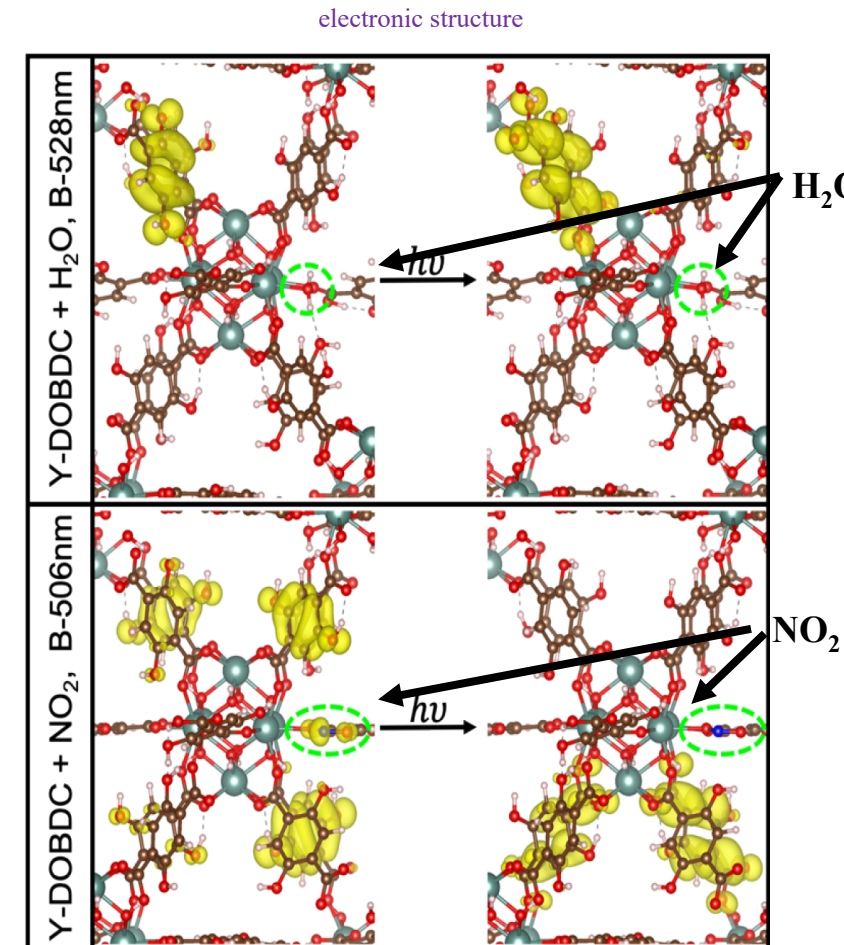
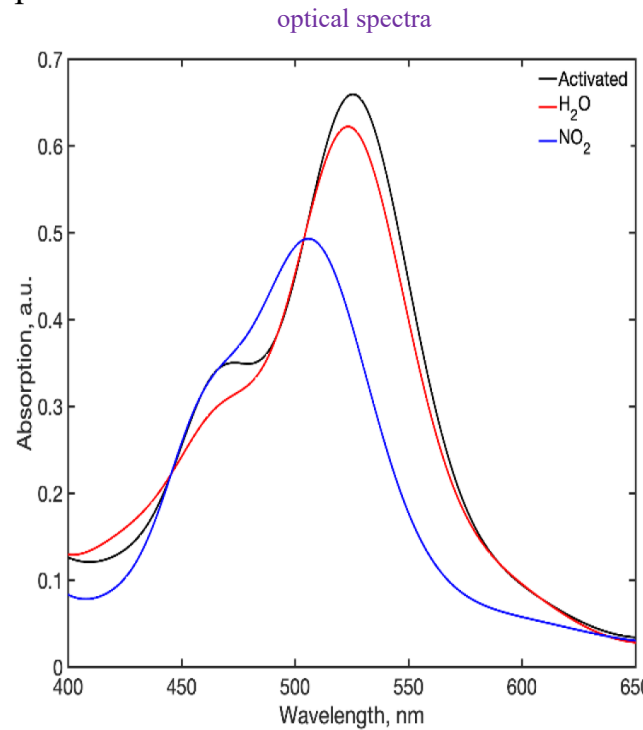
- Spin-unrestricted DFT with full 4f Valence Potential +  $U^*$
- Three different gases considered:  $\text{H}_2\text{O}$ ,  $\text{NO}_2$ ,  $\text{SO}_2$  (one molecule at a time)
- Similar strong preference for  $\text{H}_2\text{O}$  and  $\text{SO}_2$
- Different selectivity for  $\text{H}_2\text{O}$  v.  $\text{NO}_2$   $\text{NO}_x$  not as strongly bound, possible preferential ad-/desorption material
- Metal center of MOF may play an added role in gas adsorption strength (eg., Tb)

Sava Gallis, Vogel, D. J.; Vincent, G.; Rimsza, J. M.; Nenoff, T.M. *ACS Appl. Mater. Interfaces* **2019**, 11(46), 43270



# Use of DFT modeling to explain optical and electronic responses of $\text{NO}_x$ adsorption in RE-DOBDC MOF

- Experimental FTIR characterized N-O-DOBDC linkers interactions
- Calculated:  $\text{NO}_x$  adsorption shifts e-density from linkers to adsorbed  $\text{NO}_2$  molecule, reduces optical transition strength from the linkers; support exp's



Sava Gallis, Vogel, D. J.; Vincent, G.; Rimsza, J. M.; Nenoff, T.M., *ACS Appl. Mater. Interfaces* **2019**, *11*(46), 43270

# Competitive gas adsorption in RE-MOFs (binary gases: $\text{H}_2\text{O}$ , $\text{NO}_2$ )



D. Jon Vogel



Jessica Rimsza

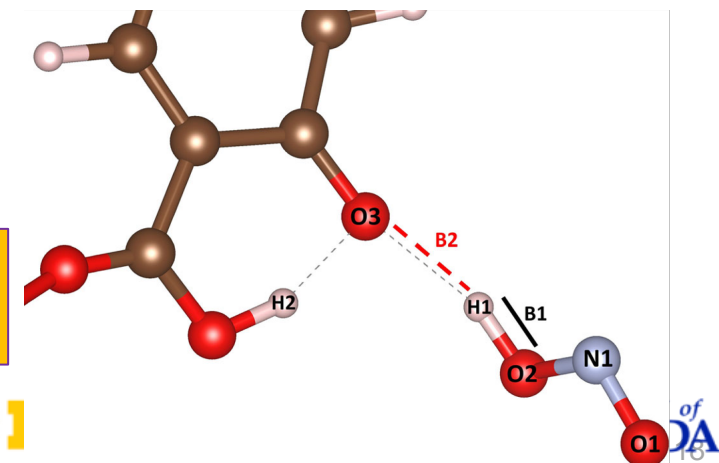
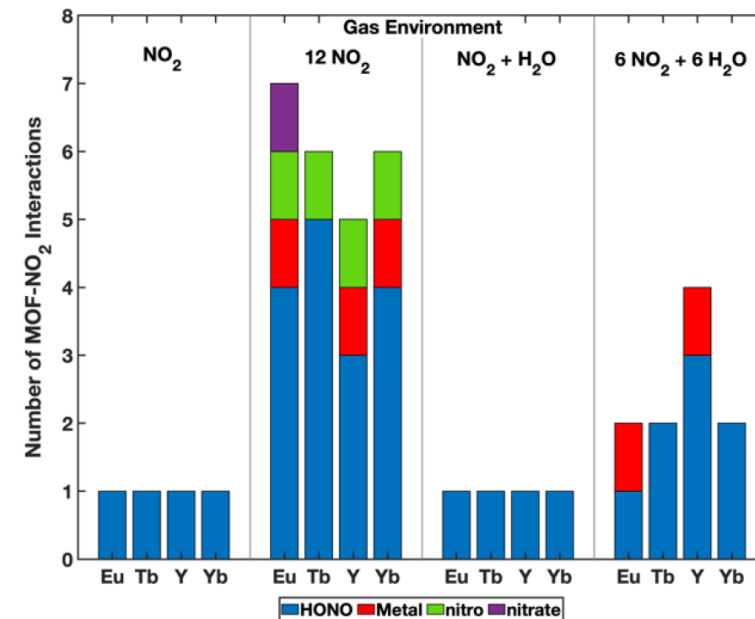
- Where and how do acid gases bind with the RE-MOF framework?
- How does competition between acid gases ( $\text{NO}_2$ ,  $\text{H}_2\text{O}$ ) impact adsorption ?

## Methods

- Static and *ab initio* molecular dynamic (AIMD) periodic density functional theory (DFT) simulations – dynamically evolving DFT trajectories
- Combination of mixed gases and elevated, ambient temperatures

## Results

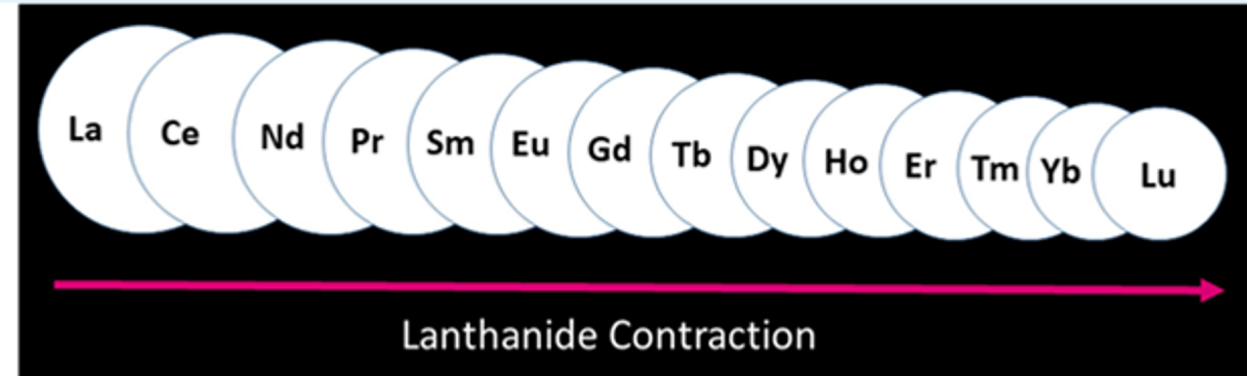
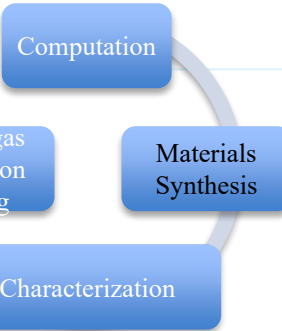
- Competitive interactions in multicomponent gases inside MOF pores decrease adsorption
- $\text{NO}_2$  preferentially binds with the ligands compared with  $\text{H}_2\text{O}$ , forming secondary molecules and nitro/nitrate species



Formation of HONO via interactions of  $\text{NO}_2$  and monodentate DOBDC linker

Invited: Vogel, Rimsza, Nenoff, *Angew. Chemie.*  
2021, 60, 20, 11514.

## II. RE-DOBDC, Entire Lanthanide Series



Henkelis, et.al., *ACS AMI*, 2021, 13, 56337



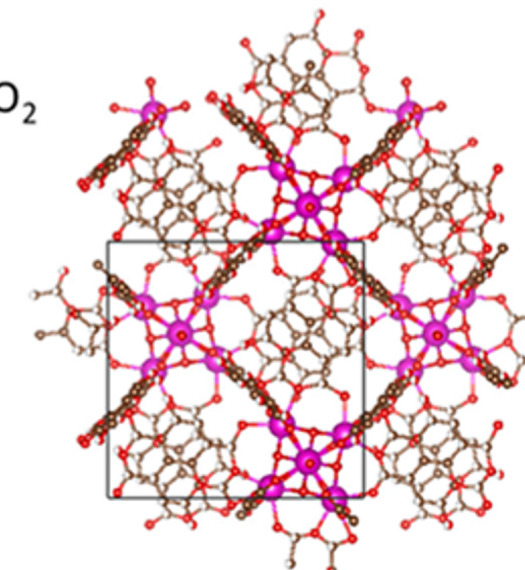
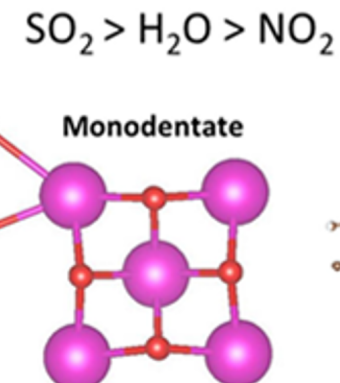
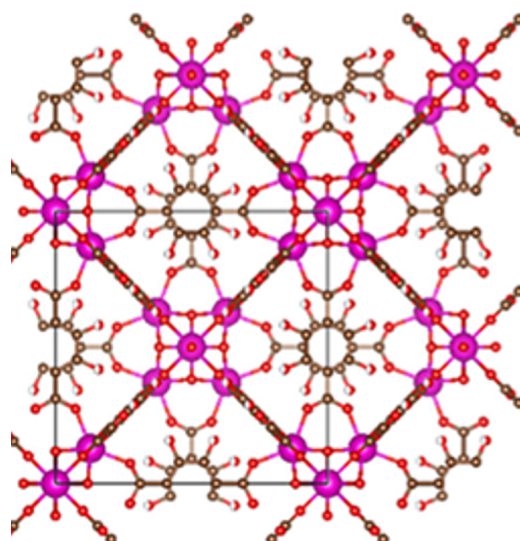
Susan Henkelis



D. Jon Vogel



Jessica Rimsza



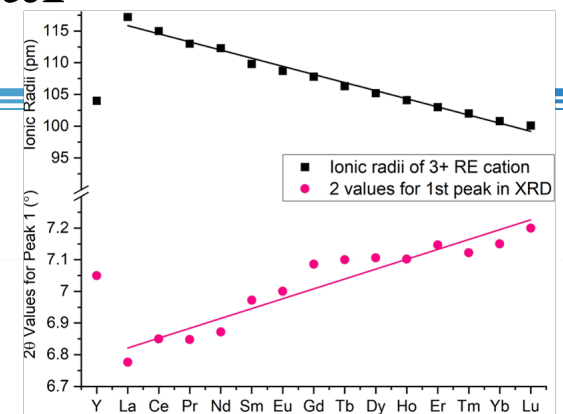
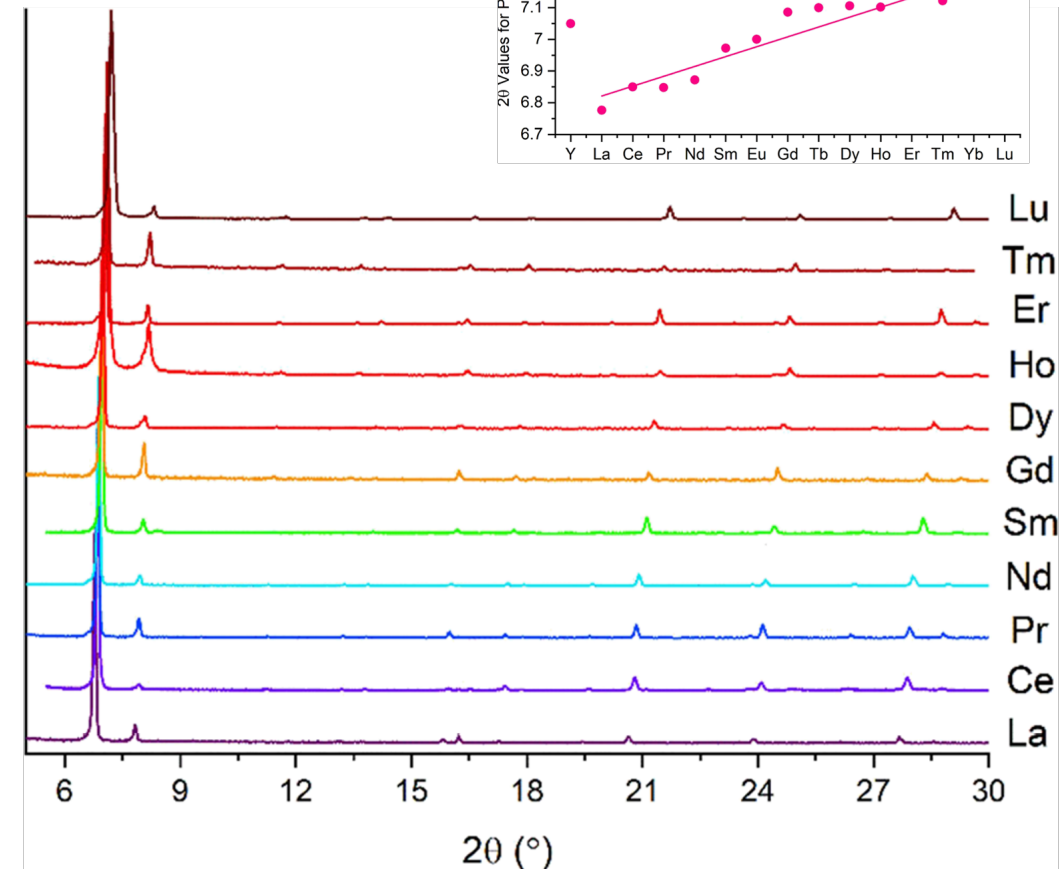
# RE-DOBDC Series: Reactions vary slightly per metal

## La-DOBDC example:

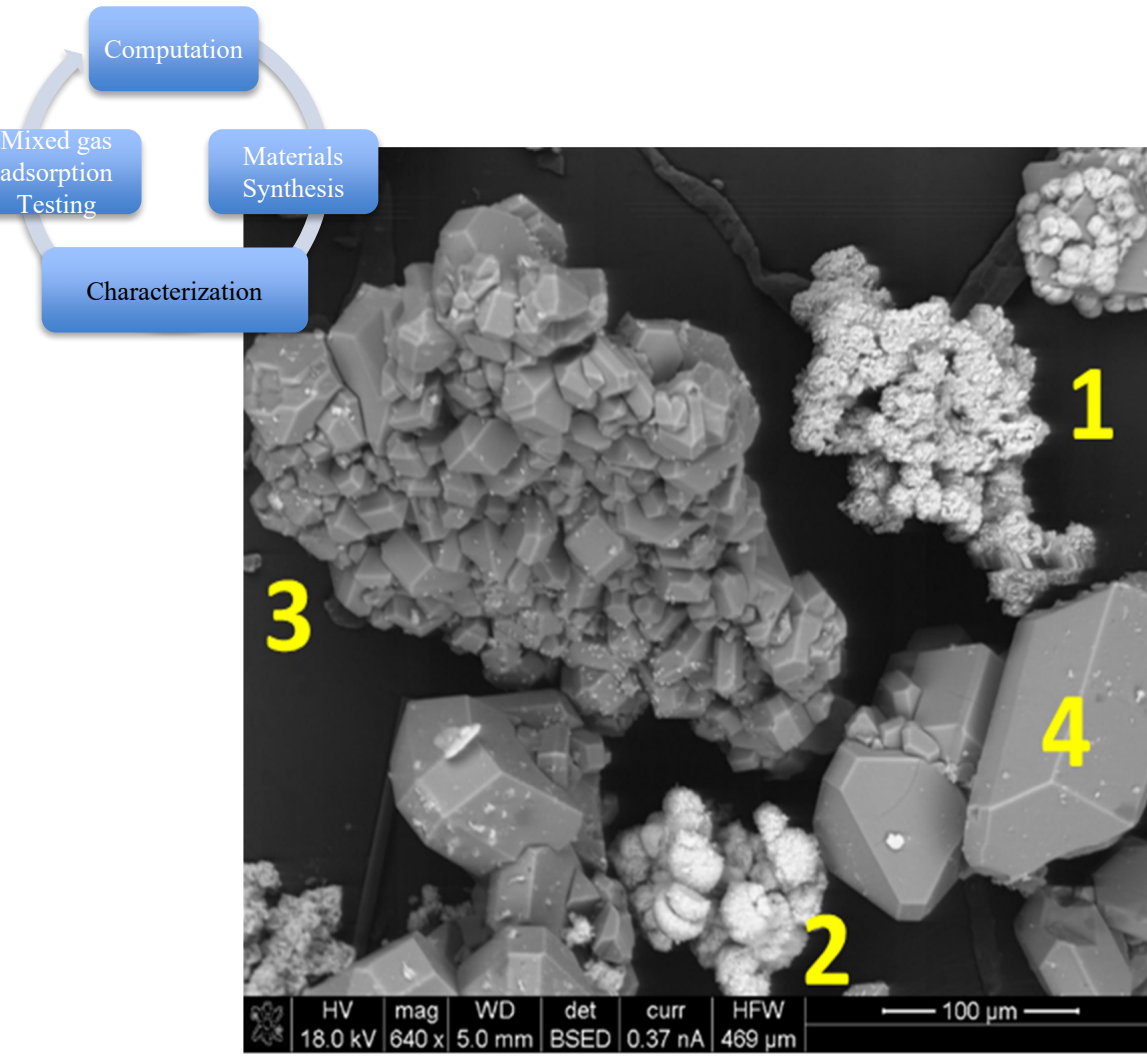
$\text{LaCl}_3 \cdot 7\text{H}_2\text{O}$  + dihydroxyterephthalic Acid + DMF  
 Dimethylformamide + DMF  
 $\text{H}_2\text{O} + \text{HNO}_3$

} 125°C, 60 hrs.

rare earth	molar ratio S:L:M	temp (°C)	days in oven
Y	1:1.32:19.84	115	3
La	1:1.46:21.86	125	3–6
Ce	1:2:21.86	125	3
Pr	1:1.46:21.86	125	6
Nd	1:1.46:21.86	125	6
Sm	1:1.46:21.86	125	3
Eu	1:1.46:21.86	115	3
Gd	1:2:21.86	125	3
Tb	1:1.46:21.86	115	3
Dy	1:1.46:21.86	125	6
Ho	1:1.58:7.98	125	3
Er	1:1.58:7.98	125	10
Tm	1:2:7.98	125	3
Yb	1:1.58:7.98	115	3
Lu	1:1.58:7.98	125	3



# SEM reveals 4 stages of crystallization in these MOFs

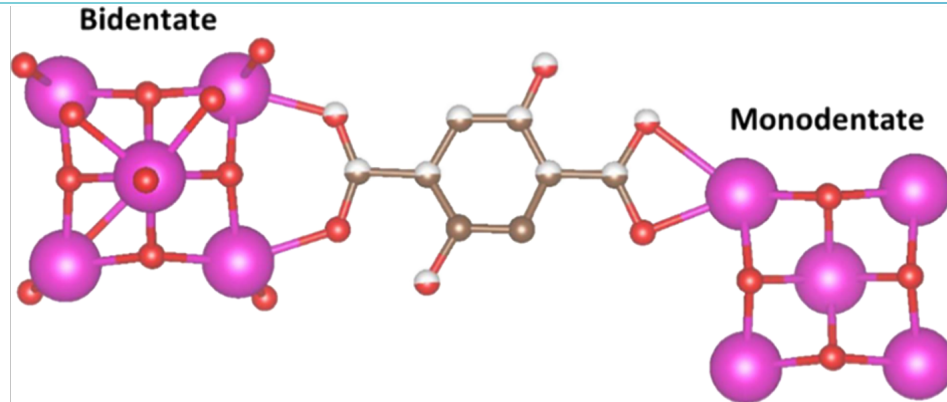


At each stage  $[M]$  decreases\*, pointing to ligand incorporation with time

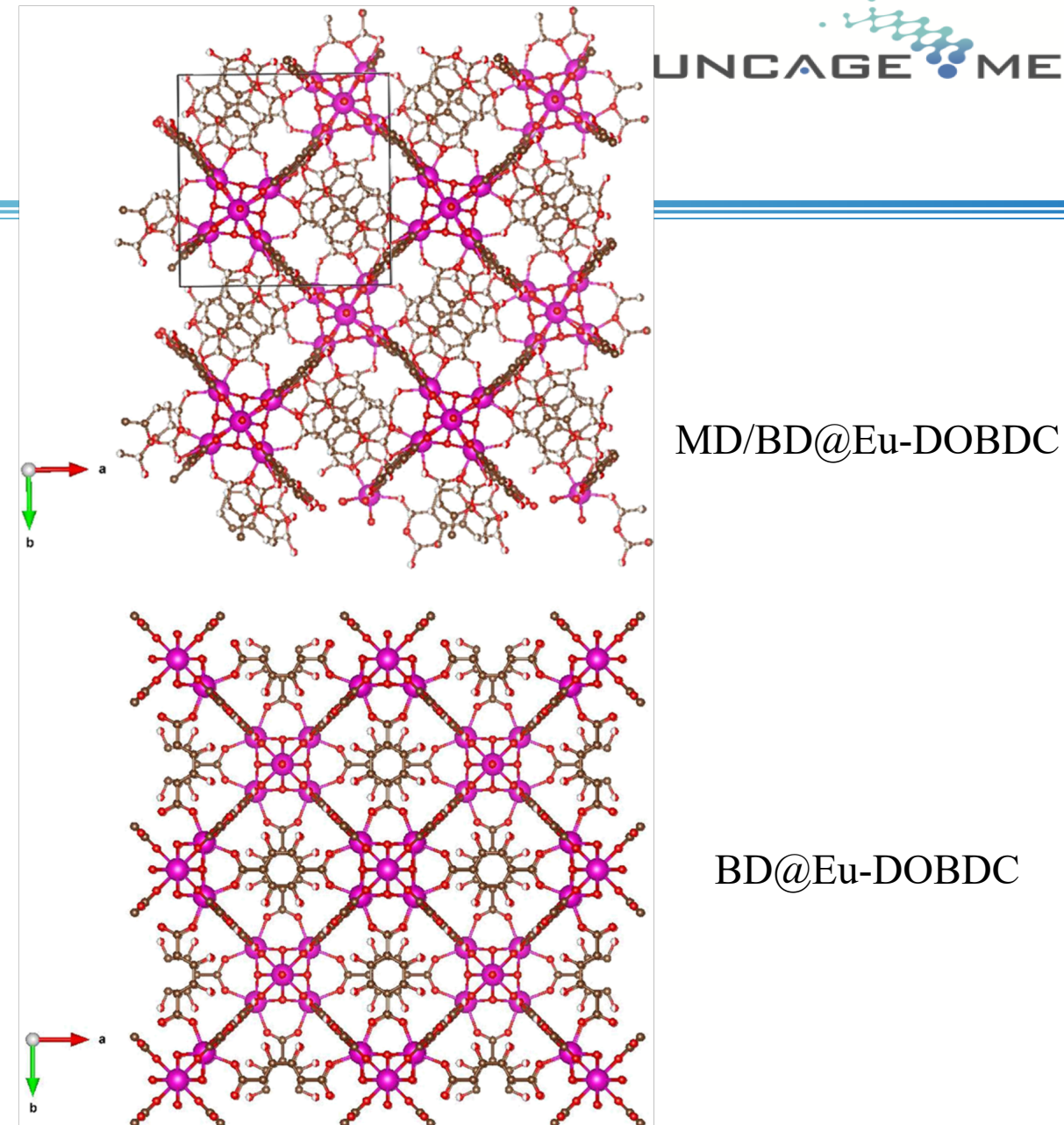
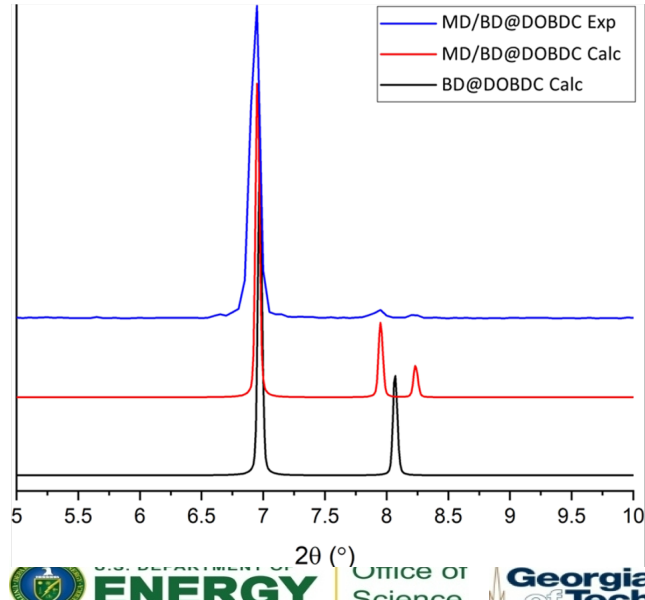
	element	Nd-DOBDC		Er-DOBDC	
		weight %	phase	element	weight %
1	Nd	91.93	nodular	Er	-
	O	8.07		O	-
2	Nd	87.56	nodular balls	Er	-
	O	12.42		O	-
3	Nd	78.10	aggregates	Er	-
	O	21.90		O	-
4	Nd	77.57	single crystal	Er	73.57
	O	22.43		O	26.43

\*Exception appears to be Er-DOBDC

# Kinetically Controlled Denticity



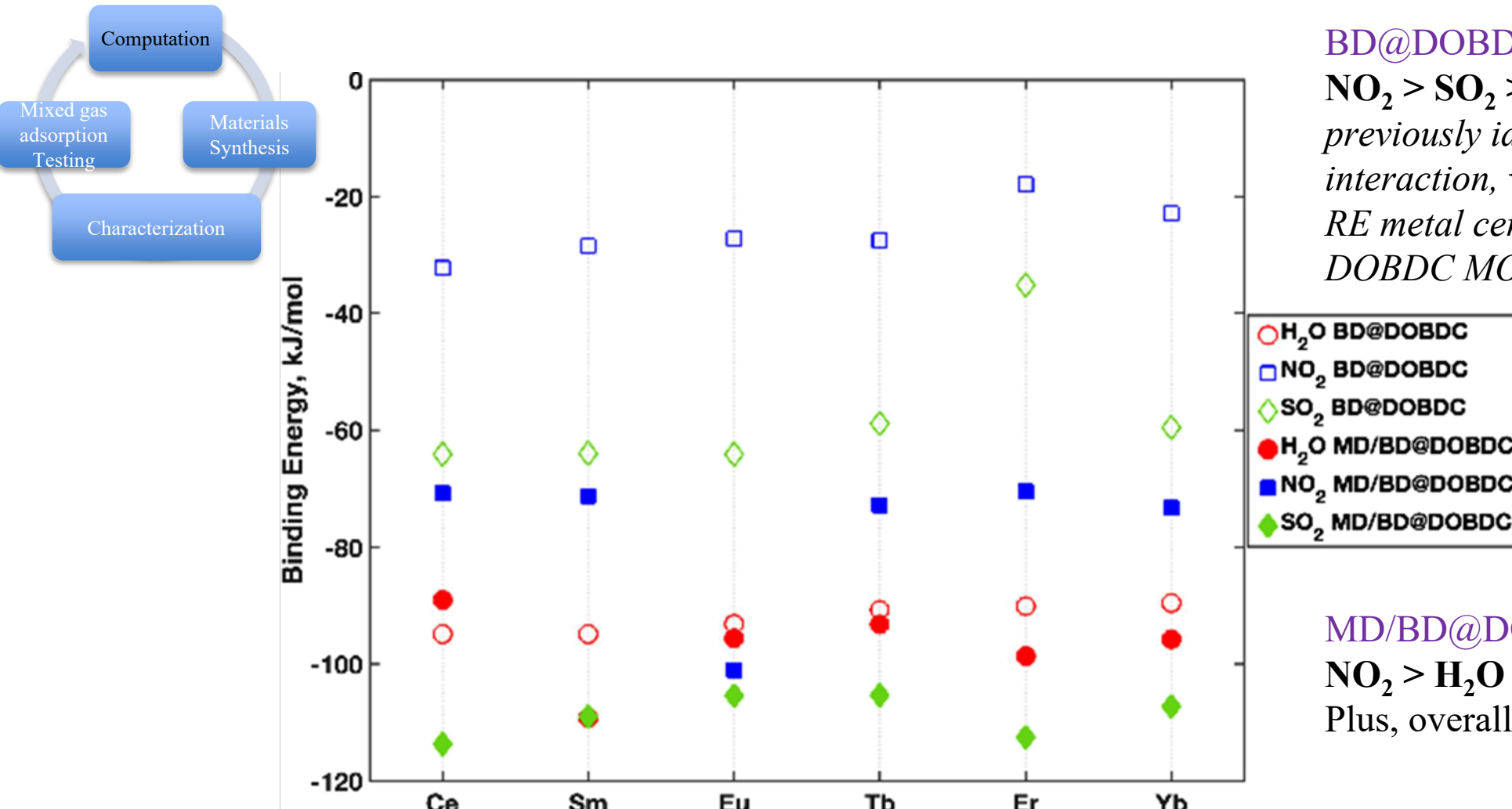
Short reaction times showed a mixture of Mono- and Bi-dentate binding of metal cluster (MD/BD-M-DOBDC)



MD/BD@Eu-DOBDC

BD@Eu-DOBDC

# Binding energies calculated indicating framework connectivity defines preferential gas binding



**BD@DOBDC MOF:**  
 $\text{NO}_2 > \text{SO}_2 > \text{H}_2\text{O}$   
*previously identified secondary H- bond interaction, when adsorbed to the RE metal center, does not form in the BD-DOBDC MOF phase.*

**MD/BD@DOBDC MOF:**  
 $\text{NO}_2 > \text{H}_2\text{O} > \text{SO}_2$   
 Plus, overall increase in binding energies

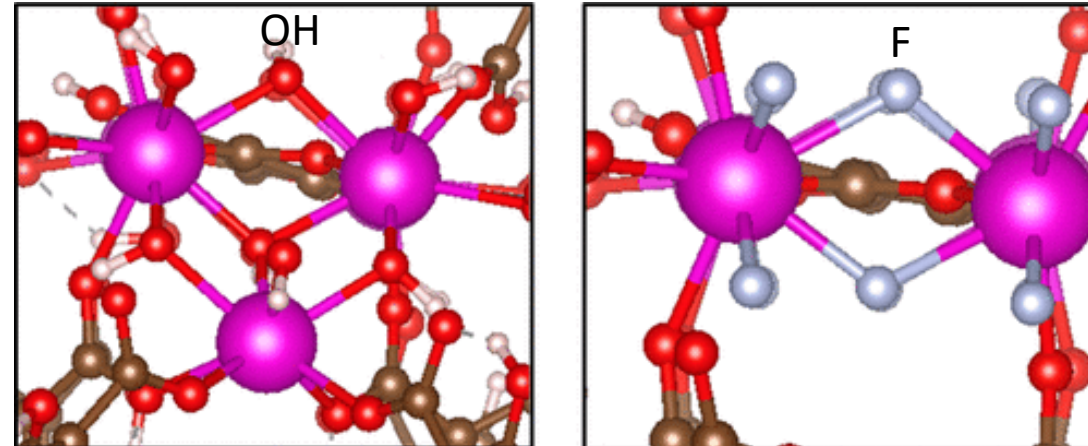
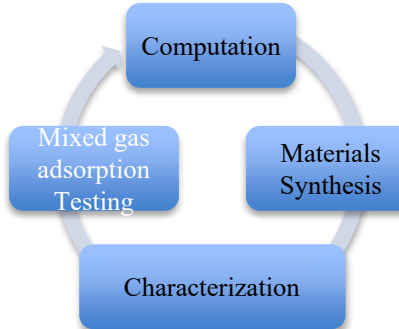
### III. Enhanced Framework Stability via Cluster Fluorination

Recently, possible fluorine doping was reported in the metal clusters in Ho-DOBDC MOF (*JACS* **2021**, *143* (43), 17995). We undertook a computational and experimental study to elucidate if fluorine incorporated into the RE-DOBDC MOFs.

VASP DFT modeling, MOF synthesis and characterization, advanced  $^{19}\text{F}$  NMR experiments

Completed for RE-DOBDC, RE-U<sub>i</sub>O<sub>66</sub>, RE(Eu)-TCPB MOFs

How: from the modulators used for crystallization of the MOFs in the reaction synthesis: *2-fluorobenzoic acid (2-fba)*



Computationally predicted fully hydroxylated RE-DOBDC MOF cluster (left)  $\mu_3\text{-OH}$  and the fully fluorinated version (right)  $\mu_3\text{-F}$



Jessica Rimsza



Matt Christian



Keith Fritzsching

# Calculated Changes of Fluorine incorporation into MOF Structures

*Computationally determined:*

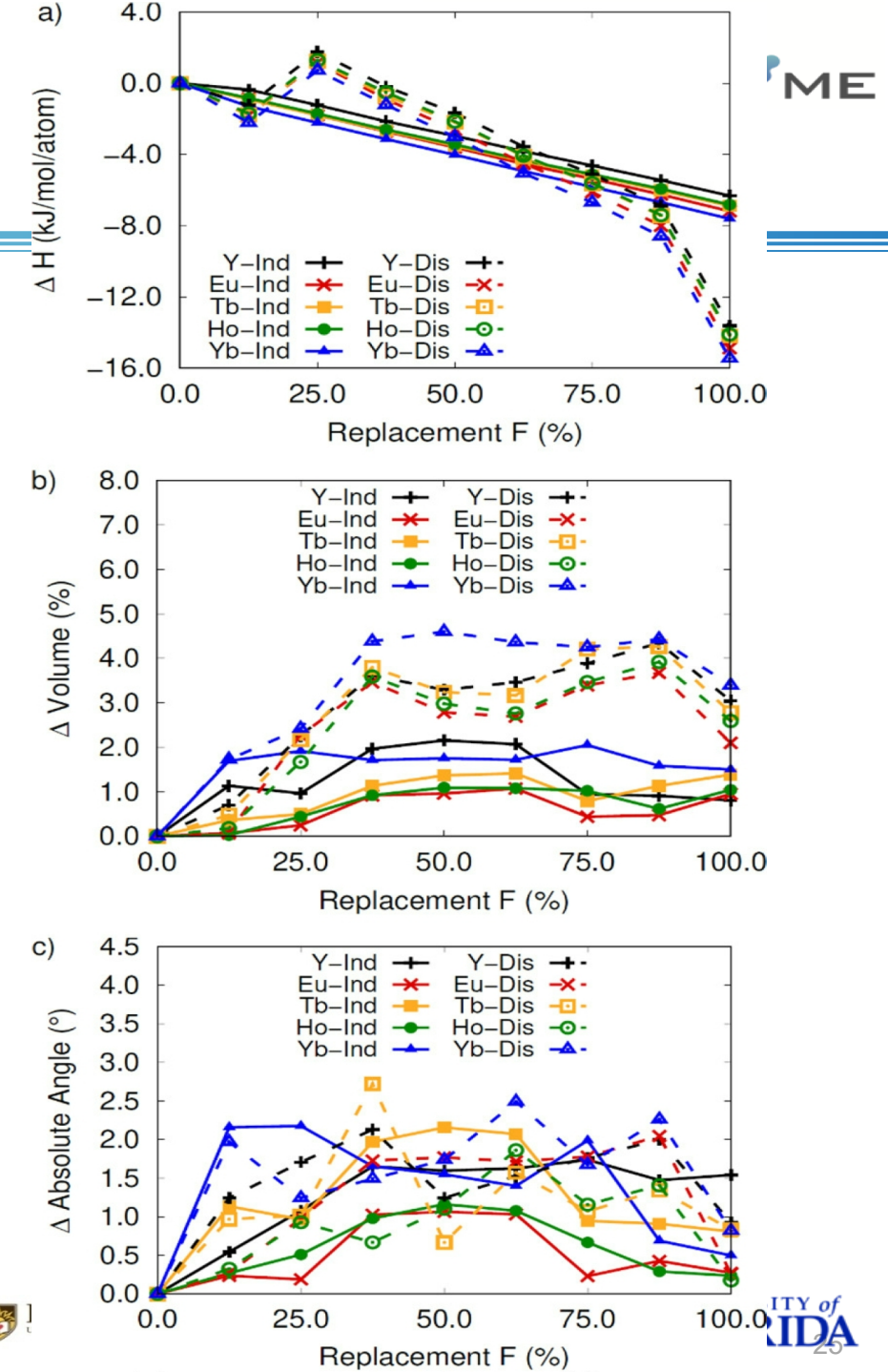
- All RE MOFs evaluated are *more stable* with the incorporation of fluorine
- Two different fluorine NMR peaks (-63 ppm, -87 ppm).

In table to right, framework topology accommodates the incorporation of F into the cluster through slide localized crystallographic changes.

(a) Change in formation enthalpy,  
(b) % volume change,  
(c) absolute sum in lattice angle change per RE atom

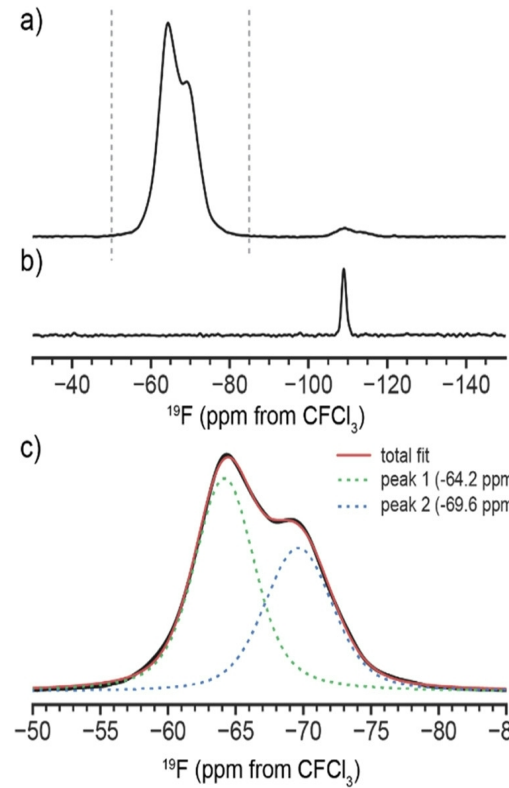
## RE-DOBDC:

Solid lines, -OH replacement on single cluster in the crystal;  
Dashed line, replacement on 2 metal clusters in crystal

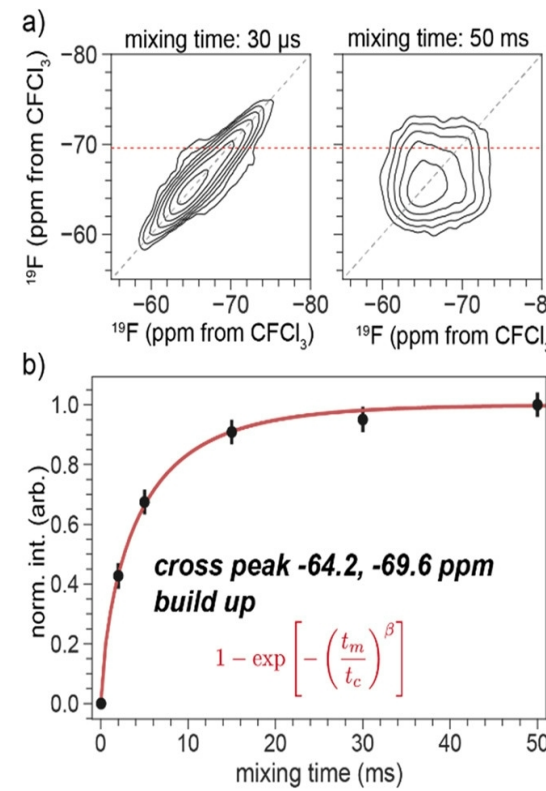


# $^{19}\text{F}$ Experiments on Y-DOBDC

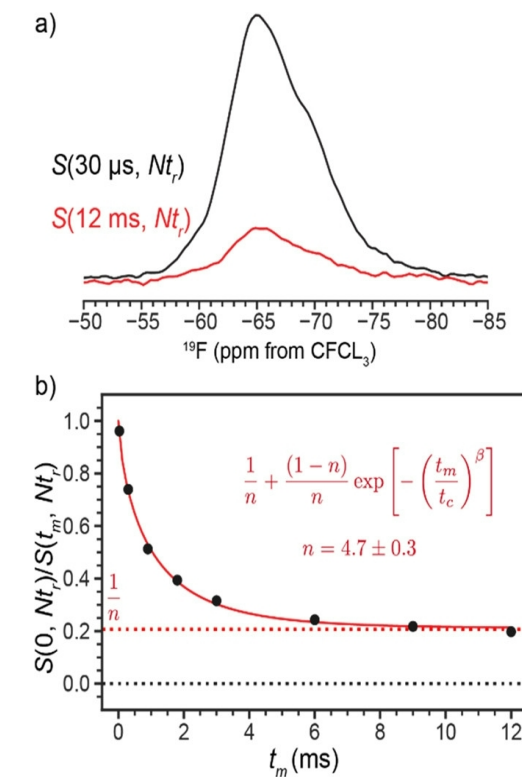
- The CODEX experiment demonstrates that  $>4$  fluorine atoms per cluster.
- Signal decays to  $\sim 0.2$  in 12 ms, corresponding to  $4.7 \pm 0.3$  ( $\pm 1\sigma$ ) nearby ( $\sim 5 \text{ \AA}$ ) fluorine spins.
- Y-DOBDC MOF structures have 8 possible fluorine sites, data indicates a fluorination rate of  $> 50\%$



$^{19}\text{F}$  NMR spectra



$^{19}\text{F}$  2D exchange NMR



$^{19}\text{F}$  CODEX NMR

# F-cluster in Y-DOBDC MOFs: no anticipated effect on Acid Gas Binding Energies and MOF Selectivities



\*calculated energies, in kJ/Mol

	H <sub>2</sub> O		NO <sub>2</sub>		SO <sub>2</sub>	
	OH	F	OH	F	OH	F
Y	-88	-83	-46	-58	-61	-57
Eu	-91	-89	-65	-67	-66	-61
Tb	-93	-89	-46	-66	-65	-62
Yb	-88	-81	-42	-54	-60	-59
Avg	-90 ± 3	-86 ± 4	-50 ± 10	-61 ± 6	-63 ± 3	-60 ± 2

RE-DOBDC MOFs retain the binding trend of H<sub>2</sub>O > SO<sub>2</sub> > NO<sub>2</sub>

Christian, M. S.; et.al., *JACS Au*, 2022, 2, 8, 1889

## IV. Use of DOBDC – based MOFs as direct electrical readout sensors



Leo Small



Mara Schindelholz



Stephen Percival



Matthew Hurlock

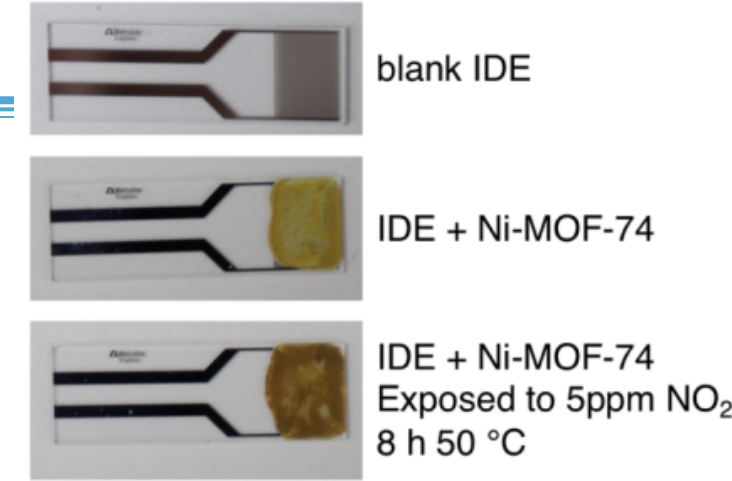


Susan Henkelis

- The ability to sense and identify **individual gaseous pollutants** from the complexity of the environment requires highly selective materials
  - Avoidance of interference from real-world air components**
- Current conductivity-based devices generally fall into two categories:
  - Solid state – (oxide based) require higher temperatures ( $>200^{\circ}\text{C}$ ) for interaction of the gas with the surface oxides; heating devices are needed
  - Fuel cell – room temperature liquid electrolyte, easily fouled, short lifetime
- Electrical **metal organic framework (MOF) based sensors** have previously been used for direct electrical sensing of gases; however, none for  $\text{NO}_2$  have been reported in open literature
- By tuning the composition of MOFs, selective chemical adsorption and/or catalysis can be achieved
- Typical sensors for this application are hard-wired or require frequent battery replacement—nanoporous MOFs allows for “near-zero” long lived sensing in a wider range of environments

# Direct Electrical Readout Sensors Combined with Nanoporous Adsorption Materials

- Composed of **Pt interdigitated electrodes (IDEs) with a nanoporous adsorbent layer**
- Nanoporous adsorption materials chosen for **ability to selectively adsorb target gas molecules**
- Electrical readout sensor of this design:
  - Decreased power consumption
  - Ability to interrogate for specified gases selectively in real-time or as an integrating sensor for delayed/later testing
- Design of an integrated sensor:
  - Record whether any **degradation product was ever present** during the sensor's lifetime
- Integrated sensor is **useful** in cases where degradation products may:
  - Subsequently **react** with other components,
  - Gradually **leak out** of the system



We have a wide study of sensors for various target gases:

*ACS Applied Mater. Interfaces*, **2017**, *9*, 44649

*Micro. Meso. Mater.* **2019**, *280*, 82

*ACS Applied Mater. Interfaces*, **2019**, *11*, 27982

*Adv. Func. Mater.* **2020**, *1407*, 2006598

*Membranes* **2021**, *11*, 176

*I&ECR* **2021**, *60*, *21*, 7998

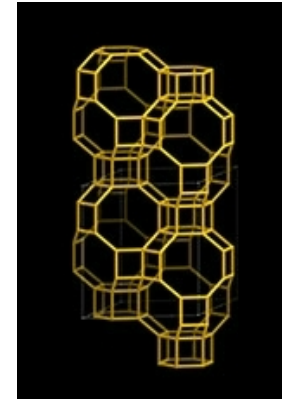
*I&ECR*, **2021**, *60*, *40*, 14371

*Chem. Soc. Rev.* **2022**, *51*, 324

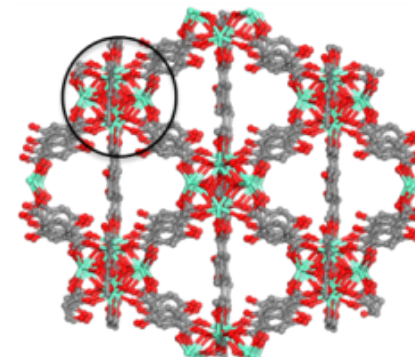
# Nanoporous Materials Targeted for the Selective Adsorption of $\text{NO}_x$

## Durable nanoporous adsorbents with selectivity for $\text{NO}_x$ at low temperatures (near ambient)

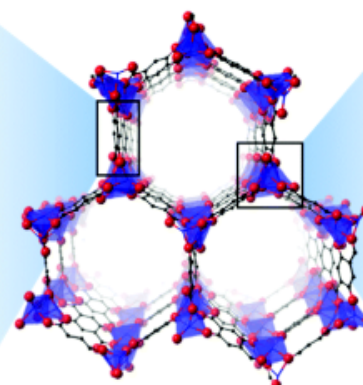
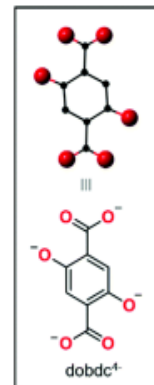
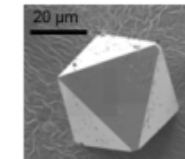
- Zeolites are aluminosilicates with high temperature durability. Specific metals give rise to  $\text{NO}_x$  selectivity
- Metal-organic frameworks (MOFs) are metal nodes with organic linkers with selectivity to  $\text{NO}_x$  designed by incorporating  $\text{NO}_x$  –friendly metals into the framework



Zeolite SSZ-13  
(CHA)



Metal-organic framework  
**M-DOBDC** (M = Y, Yb, Eu, Tb)

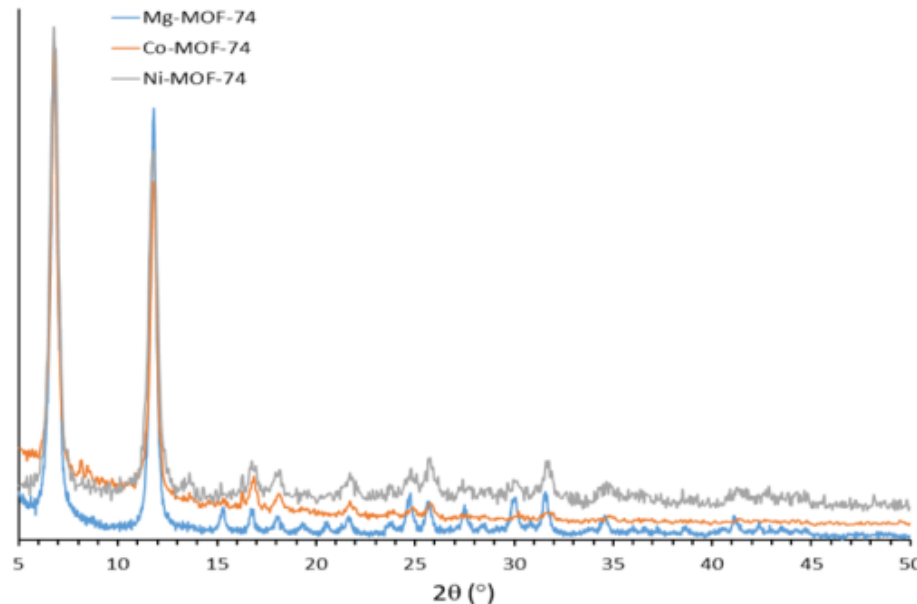


**M-MOF-74** (M = Co, Mg, Ni)  
DOBDC ligand

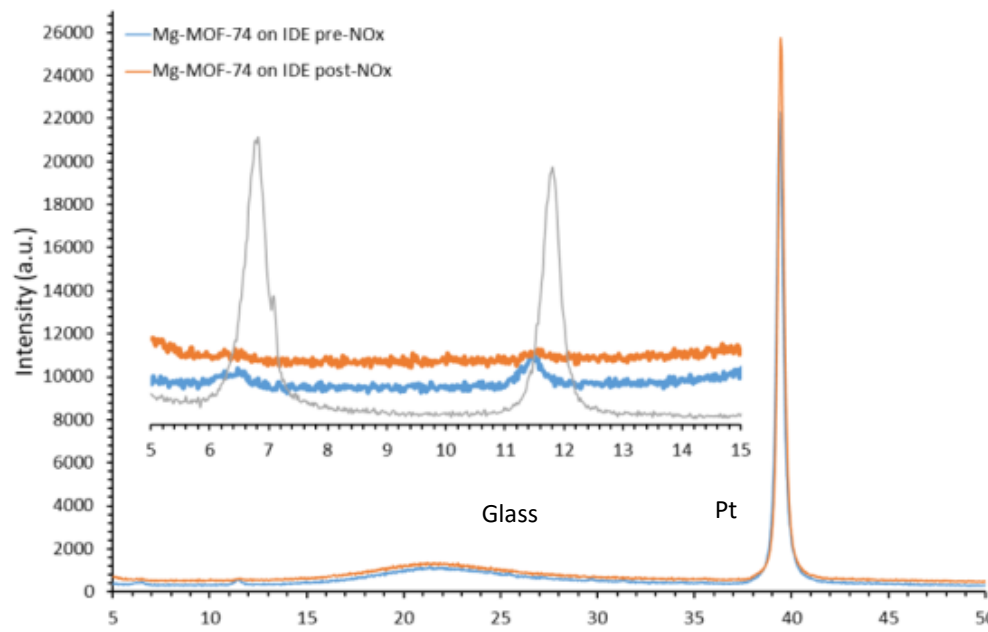
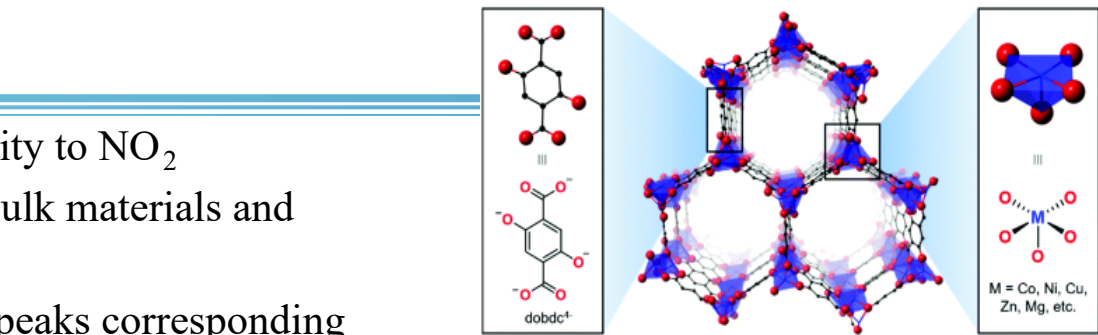
M = Co, Ni, Cu,  
Zn, Mg, etc.

# M-MOF-74-Based Sensors for the Selective Adsorption of $\text{NO}_2$

- M-MOF-74 (M= Co, Mg, Ni) was targeted for its selectivity to  $\text{NO}_2$
- MOF-74 materials were synthesized and investigated as bulk materials and dropcast onto an interdigitated electrode (IDE)
- Each powder pattern highlighted two primary diffraction peaks corresponding to the MOF pore (intensities reduced for dropcast samples, with the large peak corresponding to the platinum IDE)

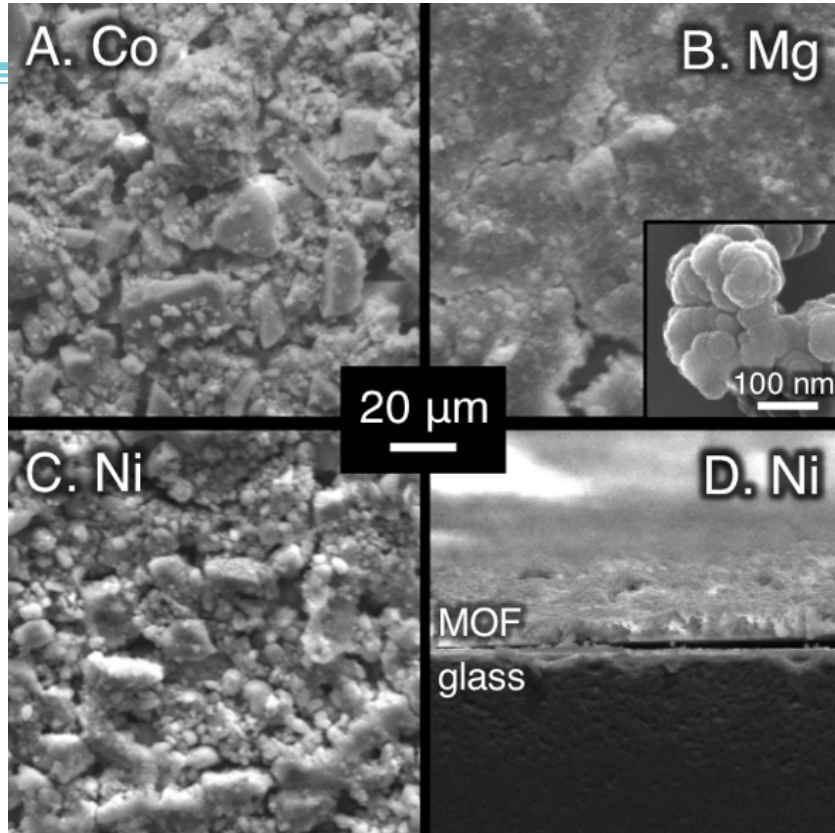


Powder XRD patterns for as-synthesized MOF-74 in the bulk phase.



Powder XRD patterns for Mg-MOF-74 dropcast onto IDE pre- $\text{NO}_2$  (blue) and post- $\text{NO}_2$  (orange). Inset: zoomed in region compared to bulk powder Mg-MOF-74.

# SEM Characterization of Dropcast M-MOF-74 Films

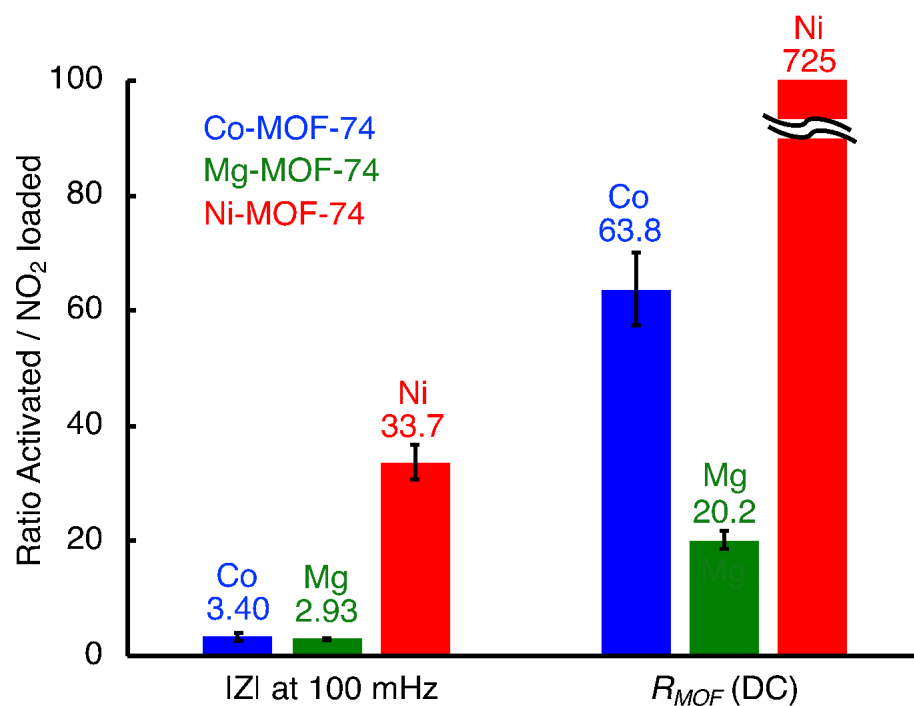


Plan-view SEM micrographs of (A) Co-MOF-74, (B) Mg-MOF-74, (C) Ni-MOF-74 powders dropcast onto IDEs. (D) Cross-sectional micrograph of Ni-MOF-74 film from (C). [

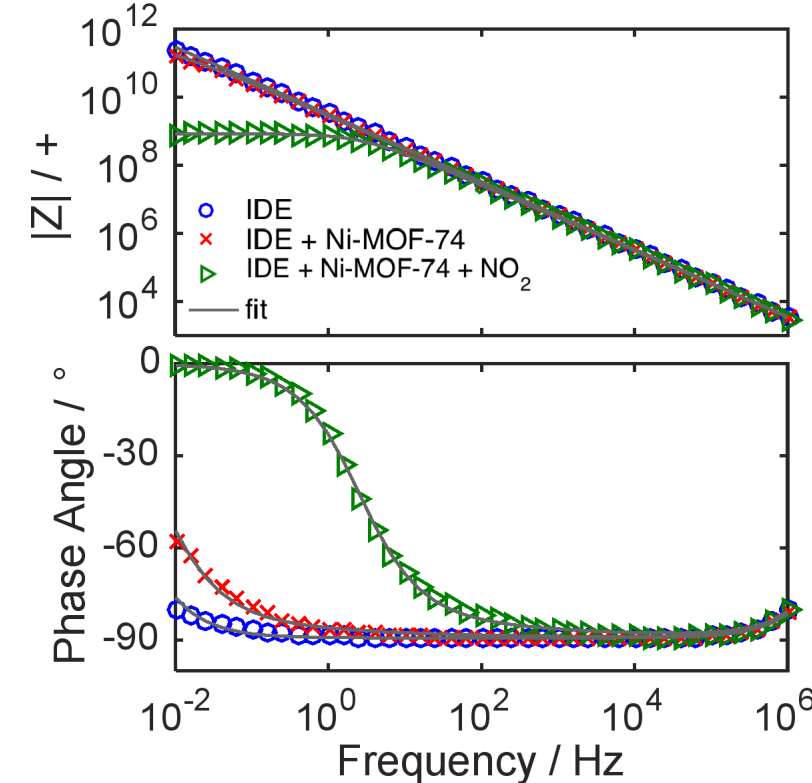
- Co- and Ni-MOF-74 contained a wide range of crystallite sizes, from 100's of  $\mu\text{m}$  to 100 nm
- Mg-MOF-74 crystallites were on the order of 100 nm
- Film thickness was  $\sim 10 \mu\text{m}$
- *Defect-free films are not necessary*

# Typical Impedance Responses of M-MOF-74-Based Sensors

Exposed M-MOF-74 (M = Co, Mg, Ni) based sensors to 5 ppm NO<sub>2</sub> for 8 h at 50°C.



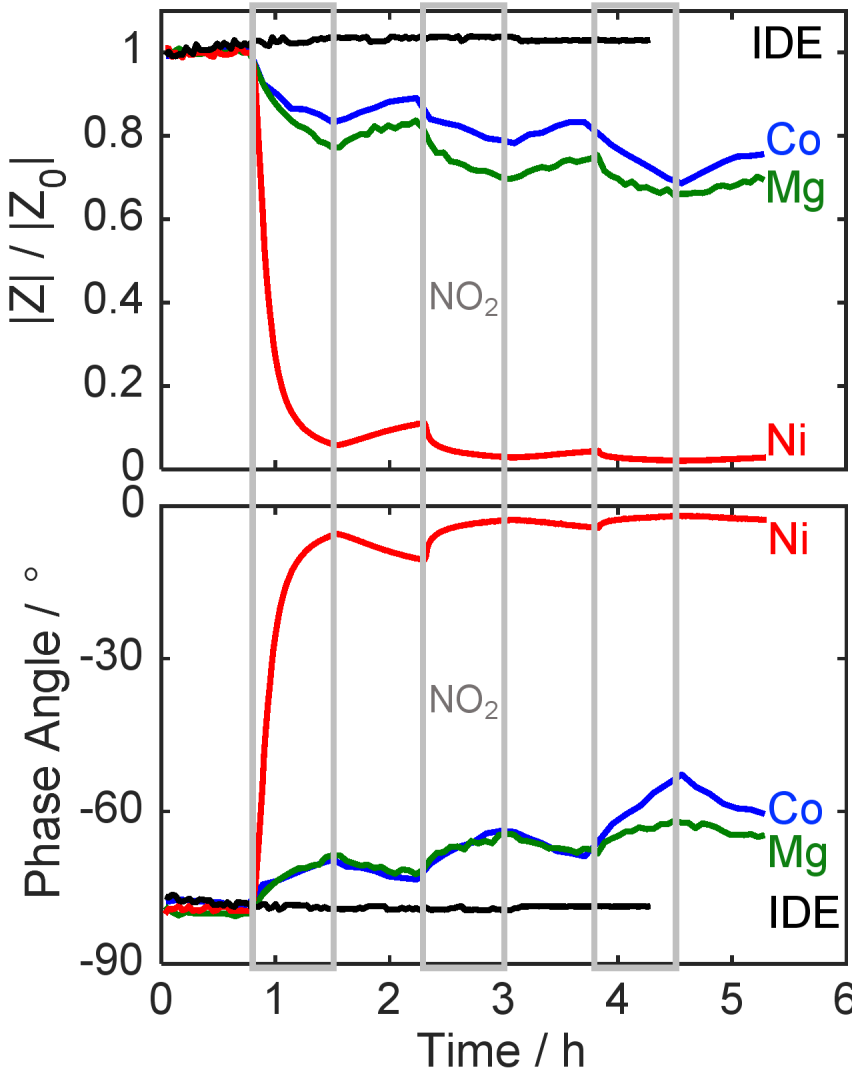
Ratio of response as-activated to NO<sub>2</sub>-exposed for (1) impedance magnitude ( $|Z_{\text{activated}}|/|Z_{\text{NO}_2}|$ ) at 100 mHz and (2) MOF DC film resistance ( $R_{\text{activated}}/R_{\text{NO}_2}$ ).



Example impedance spectra for Ni-MOF-74-based sensor

# Impedance Responses as a Function of $\text{NO}_2$ Concentration

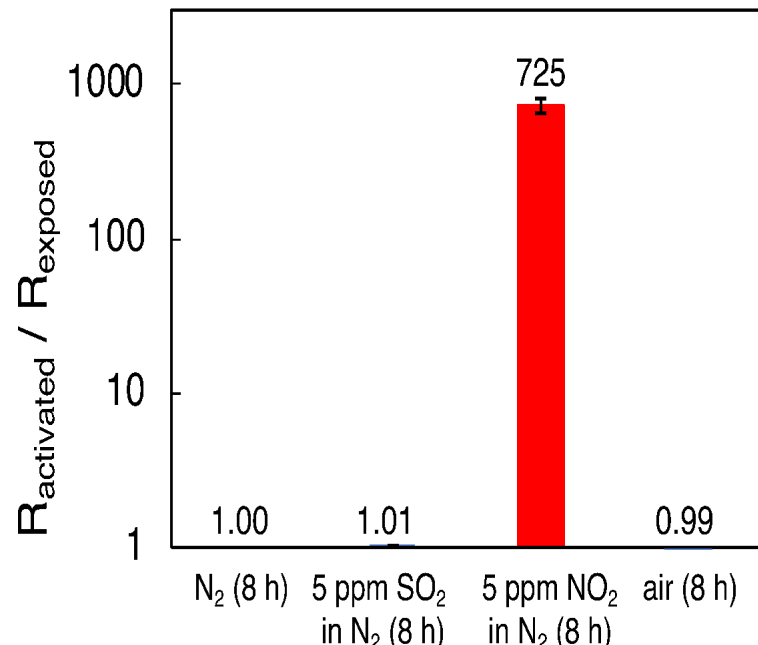
- Blank IDEs and IDEs coated in **M-MOF-74** (**M= Co, Mg, Ni**) were activated and exposed to alternating 0.75 h flows of pure  $\text{N}_2$  or  $\text{N}_2$  containing trace  $\text{NO}_2$ , while impedance was constantly measured at 100 mHz
- Magnitude of electrical response is ordered **Ni > Co > Mg**
  - Explained by each variant's  $\text{NO}_2$  adsorption capacity and specific chemical interaction
- Use of **Ni-MOF-74 provided the highest sensitivity to  $\text{NO}_2$ , with a 725 $\times$  decrease in resistance** at 5 ppm  $\text{NO}_2$  and a  $\text{NO}_2$  detection limit  $<0.5$  ppm



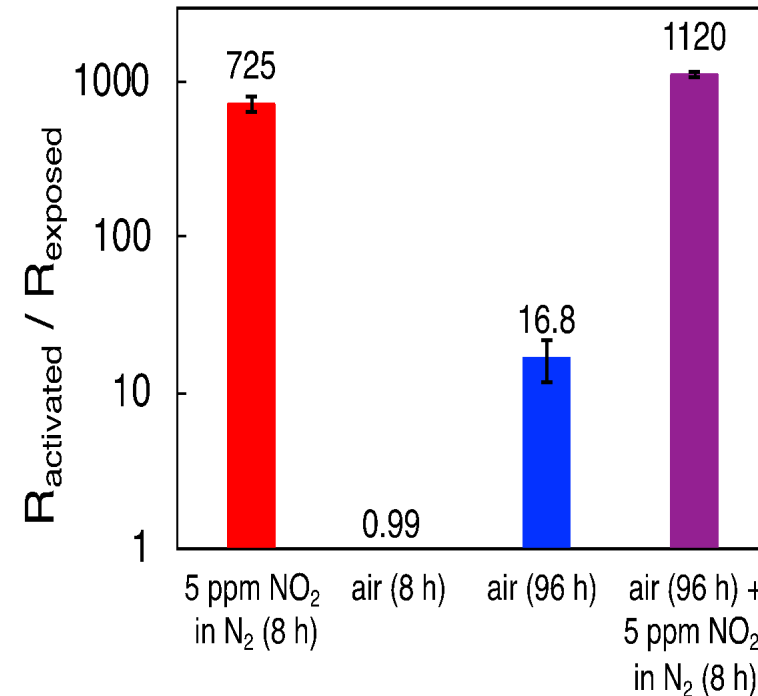
# NO<sub>2</sub> Selectivity for a Ni-MOF-74-Based Sensor

- A Ni-MOF-74-based sensor was activated and exposed to 5 ppm SO<sub>2</sub> in N<sub>2</sub>, and ambient air (25 °C, 50% RH, 400 pm CO<sub>2</sub>) heated to 50 °C, and its response compared to previous exposures to 5 ppm NO<sub>2</sub> in N<sub>2</sub>
- An extended air exposure (96 hours) followed by subsequent NO<sub>2</sub> exposure was also performed
- The Ni-MOF-74-based sensor demonstrated selectivity to NO<sub>2</sub> versus N<sub>2</sub>, SO<sub>2</sub>, and air.

**A. Ni-MOF-74**

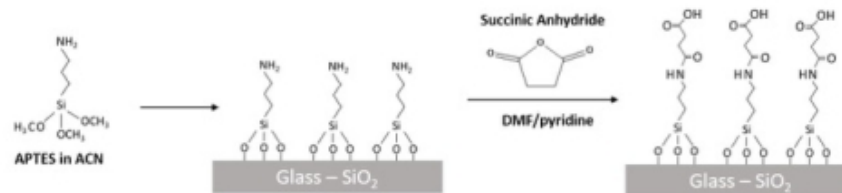


**B. Ni-MOF-74**

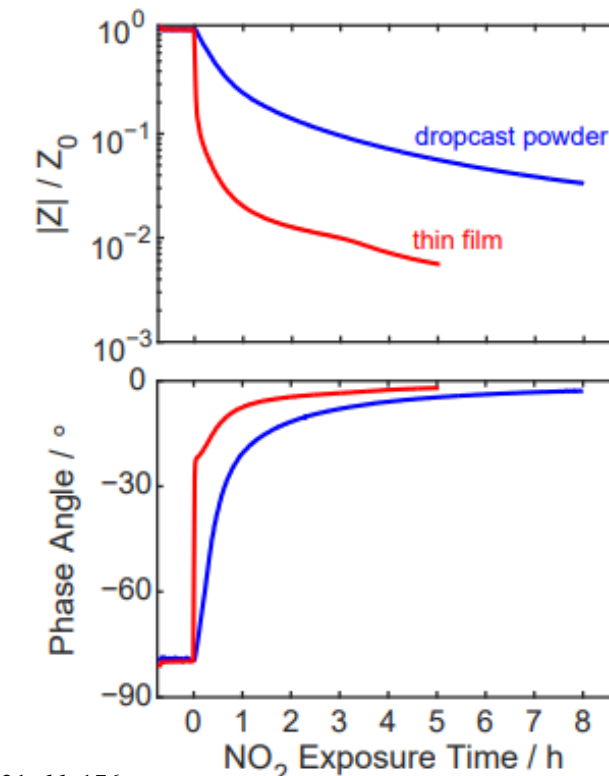
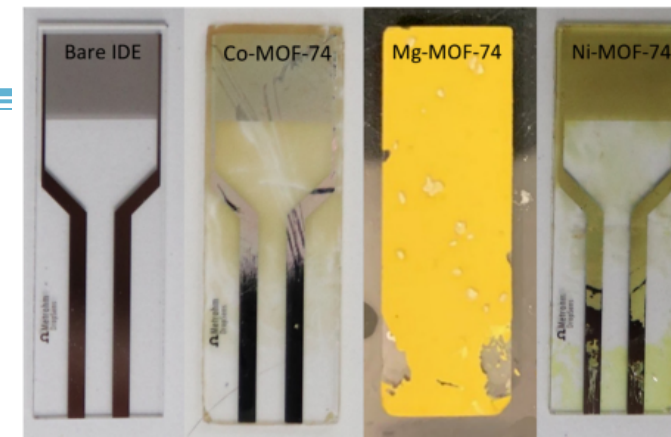


# Enhanced Sensitivity of Nanoporous-Based Sensors Using MOF Thin Film Membranes

- M-MOF-74 (M=Co, Mg, Ni) MOFs synthesized as crystalline thin films on functionalized IDEs
- *Two step functionalization procedure*:
  - Reacted IDE with aminosilanes, followed by ring opening of succinic anhydride
  - Functionalization allowed for binding of metal cation and further growth of 3-D MOF

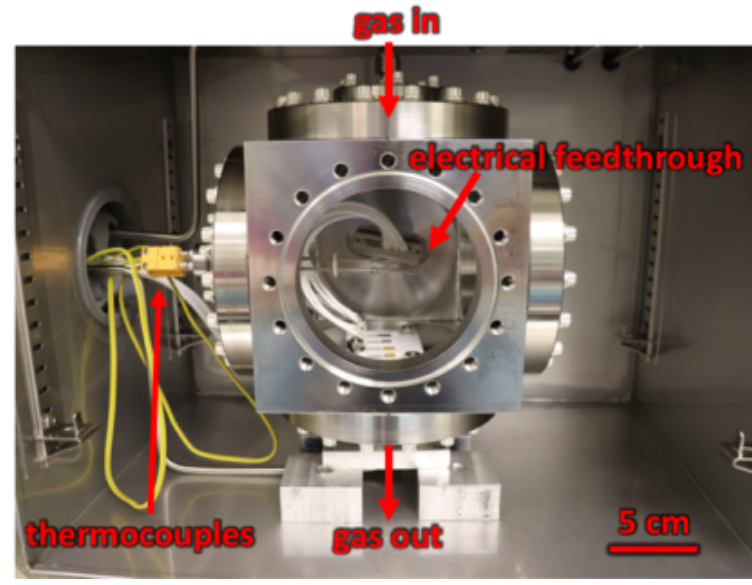


- Ni-MOF-74 boasted a continuous thin film and used in a comparison study vs. a dropcast powder
- Thin film passed a modified **ASTM D3359** test for durability
- Thin film membranes resulted in an increased response rate and larger total change in impedance

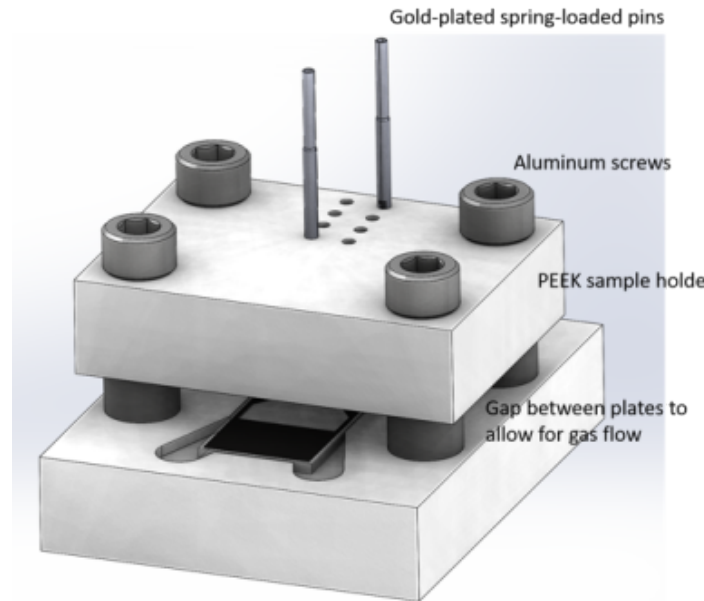


# NO<sub>x</sub> Exposure and In Situ Electrical Testing

- Custom- built NO<sub>x</sub> exposure chamber enabled Zeolite, MOF activation and subsequent in situ electrical testing under varying NO<sub>2</sub> concentrations without exposure to lab atmospheres
- Variable NO<sub>2</sub> concentrations (0.5 - 5 ppm) were achieved by diluting 5 ppm NO<sub>2</sub> gas stream with pure UHP N<sub>2</sub> at 500 sccm total gas flow
- Impedance spectra recorded at 0 V DC and 100 mV (RMS) AC over 1 MHz - 10 mHz
- All electrical measurements and NO<sub>2</sub> exposures occurred at 50°C

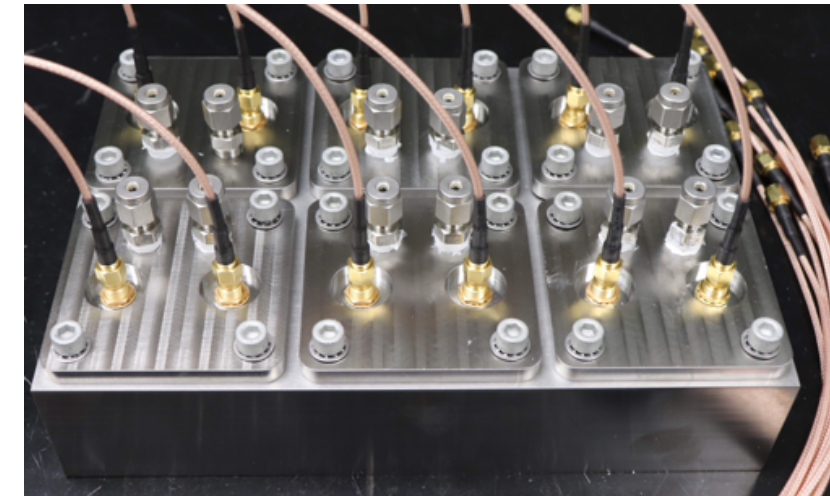
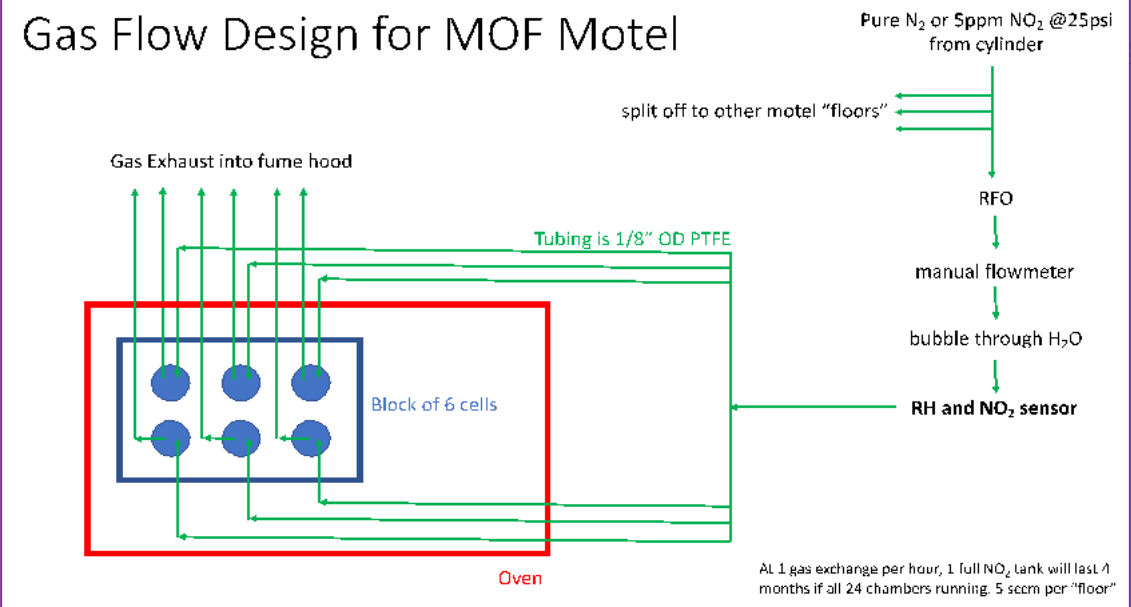


# Custom Test Fixtures for Multiple & Simultaneous Long-Term Exposure and Electrical Testing



- Custom designed test fixtures ('MOF Motel') for long-term exposures and in-situ electrical testing of sensors
- 24 test cells, each cell 70 mL
- Humidity/NO<sub>x</sub> levels controlled in each chamber with constant temperature across entire test fixture

## Gas Flow Design for MOF Motel



# RE-DOBDC MOF: Conclusions, Highlights and Future Research



## We have successfully established

Structural stability of Sandia RE-DOBDC MOFs to  $\text{NO}_x$  &  $\text{SO}_x$  acid gas and humidity, RE: Y, Eu, Tb, Yb

The ability to retain the coordination geometry (cluster) across of series of rare earth elements

This control of the building block is rare in MOFs in a series

Use of modeling and experiment confirmed Fluorine incorporation into RE-DOBDC, RE-U<sub>3</sub>O<sub>6</sub>6, and RE-TCPB MOFs

Use of modulator in crystallization reaction is the source, *2-fluorobenzoic acid (2-fba)*

No anticipated affects on binding preference to the metal by various acid gases, due to shielding of the F by the metals

**Application** use established for industrial and automotive caustic gas detectors, highly tunable and selective for gases of interest even with competing air gases

## Future / On-going Research:

**Accelerate Materials Discovery:** Design next generation caustic gas stable adsorbents (MOFs and Zeolites) from DFT/AIMD modeling predictions with associated synthesis, characterization and testing

Transitioning into the computational design and synthesis of porous liquids and carbons for enhanced greenhouse gas selectivity

# Best Team!

## SNL Postdocs, Interns/students, Technologist and Young Staff\*

*Strong Advocate for Mentoring and Supporting Young People throughout their Careers*

### Postdocs



Matthew Hurlock,  
postdoc 1874



Matthew Christian  
Postdoc 8915



D. Jon Vogel  
Staff SNL 1864



Dorina Sava Gallis  
Staff SNL 1874



Koroush Sasan  
Staff LLNL



Z. Mark Zhang  
Dept. of Interior



Summer Ferreira,  
Manager SNL 8812



Susan Henkelis,  
LTE SNL 5228

### Postdocs, not shown

Genoveva Buelna, ACS  
François Bonhomme, CNRS  
Ranko Bontchev, Cabot

### Interns, not shown:

Alejandra Chavez, Dow Chemical  
Sarah Moore, Chevron  
Sera Mirchandani, AECOM



Marie Parkes,  
LTE SNL 8915  
Consultant



Nathan Ockwig  
3M Corp.



Jason Pless,  
Johnson Matthey



Mutlu Kartin,  
Staff SNL 8367,  
Prof. Dominican Univ



Andrea  
Ambrosini,  
Staff SNL 8923



Margaret Gordon,  
Manager SNL  
8923



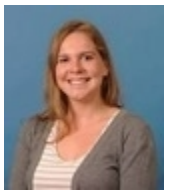
May Nyman,  
Staff SNL 8915  
Prof. Oregon State



Jessica Rimsza  
SNL 8915

### Young Staff FY19-23\*

### Interns



Haylie Lobeck  
NNSA FPM NA-192  
Office of Tritium and  
Domestic U Enrichment



Jackie Unangst  
General Atomics



Melissa Teague  
Staff SNL1832  
(On leave)



Jesse Stanchfield  
Intel Corp



Sylvia Hanna  
NNSA Graduate Research  
Fellow (SNL 1874)  
Northwestern Univ.

### Technologist



David Rademacher  
DNTG 1874



Remi Dingreville  
SNL1881



Mara Schindelholz  
SNL 2491



Stephen Percival  
SNL 1816



Leo Small  
SNL 1874

# Acknowledgements

## Funding:

This work was supported as part of the Center for Understanding and Control of Acid Gas-Induced Evolution of Materials for Energy (*UNCAGE-ME*), an Energy Frontier Research Center, funded by the U.S. Department of Energy (DOE), Office of Science, Office of Basic Energy Sciences (BES) under Award DE-SC0012577.

## Sandia National Labs:

Jessica Rimsza  
D. Jon Vogel (pd)  
Matt Christian (pd)  
Susan Henkelis (pd)  
Matthew Hurlock (pd)  
Dorina Sava Gallis  
Grace Vincent (undergrad)  
Kennedy Block (HS intern)  
Mark Rodriguez  
Nichole Valdez  
Dale Huber (CINT/SNL)  
John Watt

## ORNL/SNS, Univ. TN:

Katharine Page  
Stephen Purdy (pd)

## Univ AL:

David Dixon  
Zachary Lee (grad student)

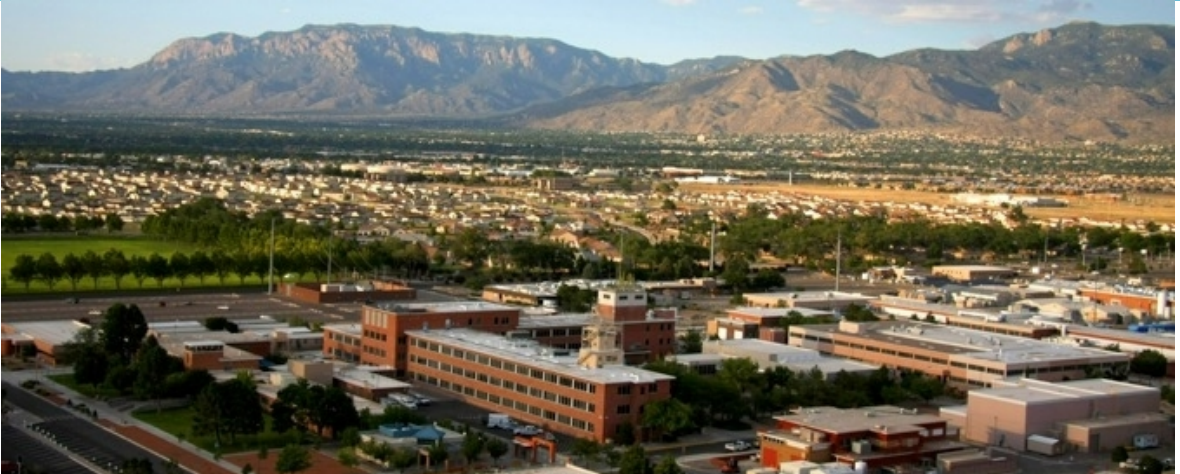
## GA Tech:

Krista Walton  
Ian Walton (pd)  
Ryan Lively  
Chunyi Li (grad student)  
Stephen Dewitt (grad student)

## Stonybrook University:

Karena Chapman

# Sandia National Laboratories



Albuquerque, New Mexico



Livermore, CA

Sandia, an US/NNSA lab  
~\$3.8B/yr, 14,000+ employees  
Engineers and Scientists  
Fiscal year Oct 1 – Sept 30  
Staff, postdocs and fellowships  
<http://www.sandia.gov/careers>



Kauai Test Facility  
Hawaii



Tonopah Test  
Range, Nevada



Yucca Mountain,  
Nevada



WIPP,  
New Mexico



Pantex, Texas

# Questions? / Thank you



*UNCAGE-ME*  
SNL Team,  
Sandia Peak  
(10,679'),  
NM. 2019



*UNCAGE-ME*  
SNL Team, *IZC*,  
Valencia, Spain  
2022

# Extra Slides

## IV. Use of DOBDC – based MOFs as direct electrical readout sensors



Leo Small



Mara Schindelholz



Stephen Percival

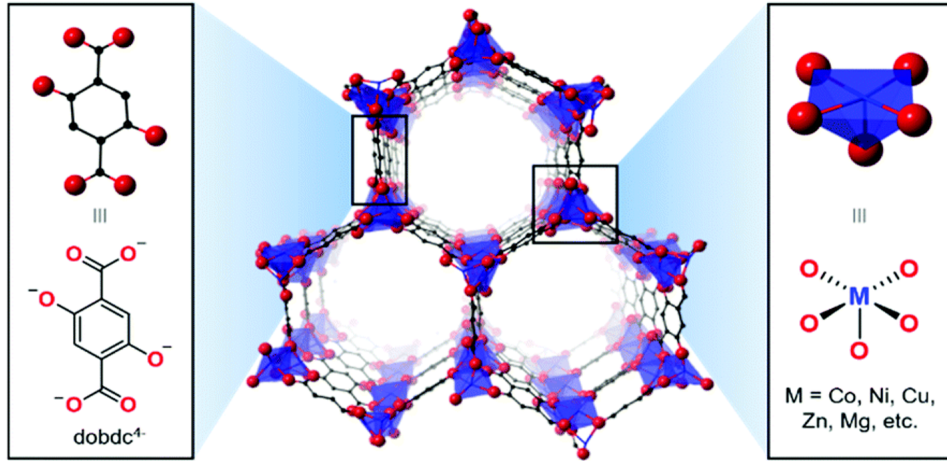


Matthew Hurlock



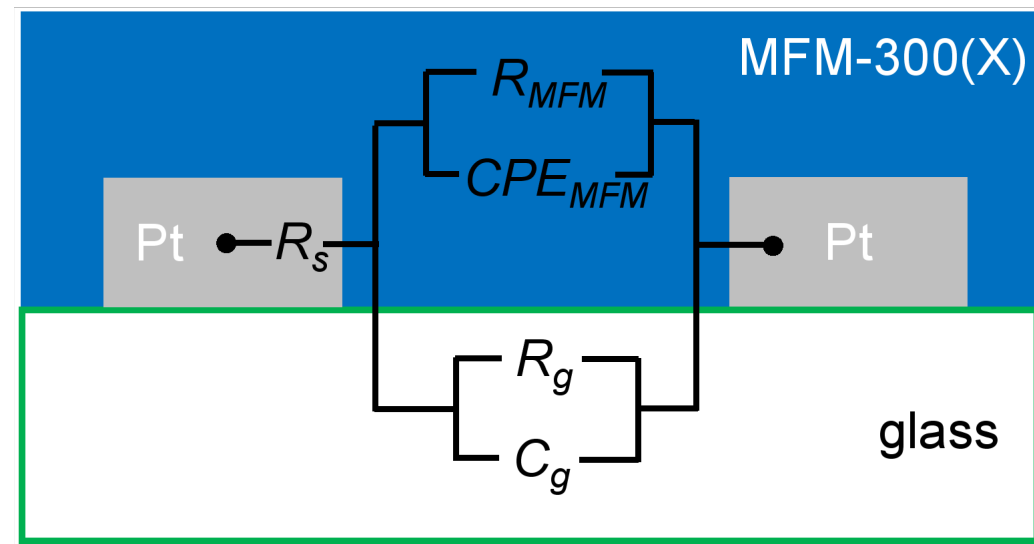
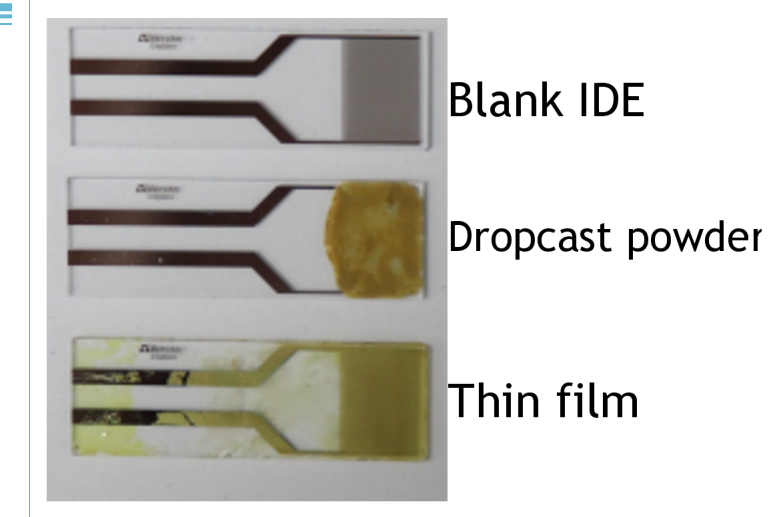
Susan Henkelis

We have successfully used DOBDC based highly tuned gas sensors, useful in complex gas streams



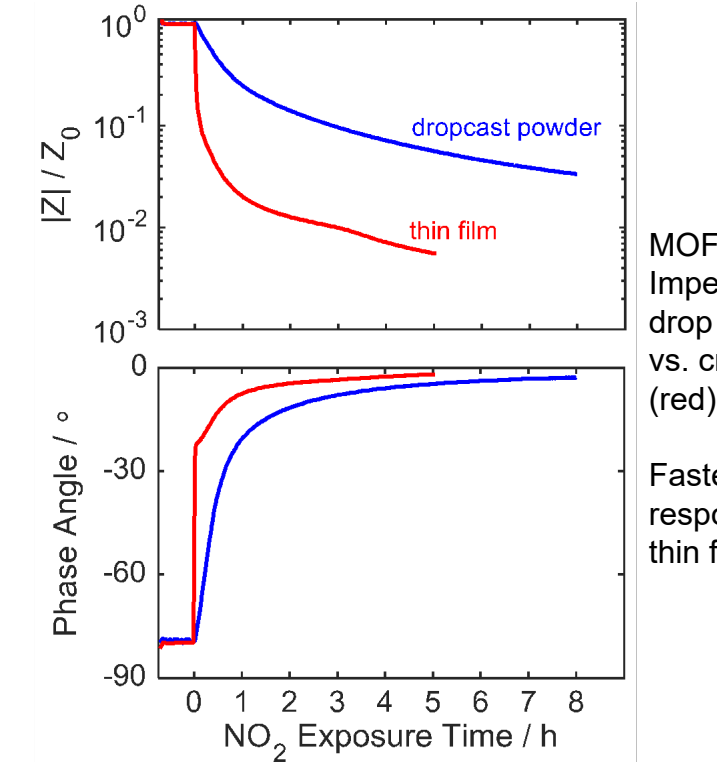
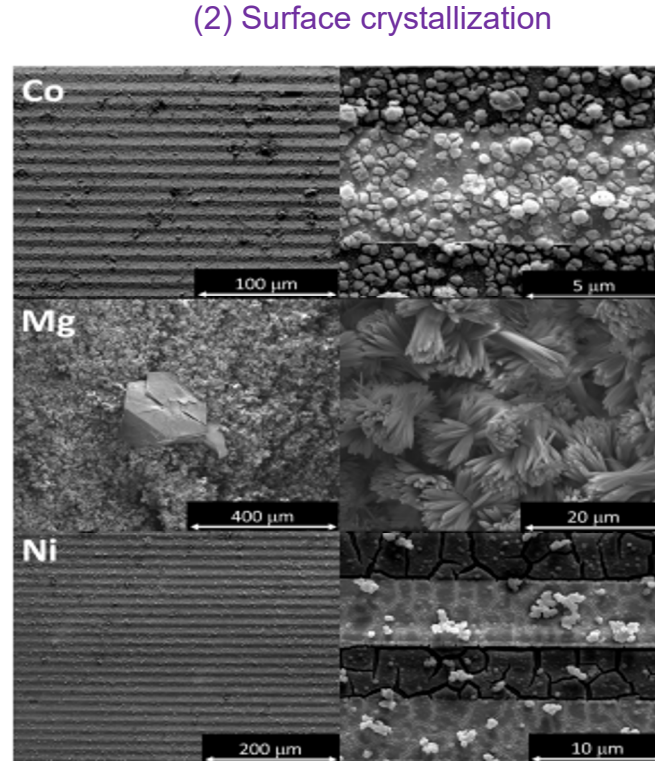
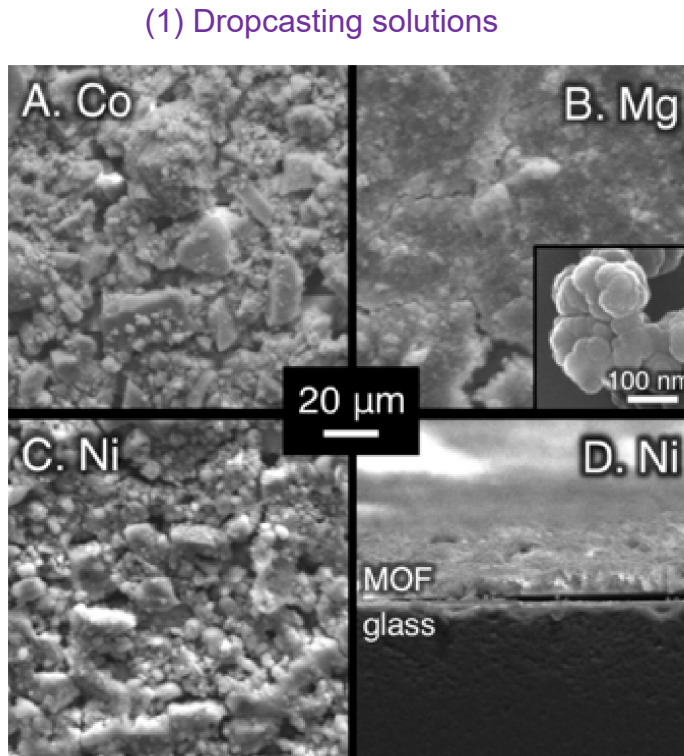
One example:  
M-MOF-74; M = Ni, Co, Mg

*Gas binding inside the MOF  
and charge transfer enables the  
sensor response*



# MOFs provide the selectivity to the target gas to be detected

Judicious choice of MOF or Zeolite for gas of interest. Thin film fabricated on interdigitated electrode (IDE). M-MOF-74 membranes fabricated by two methods:



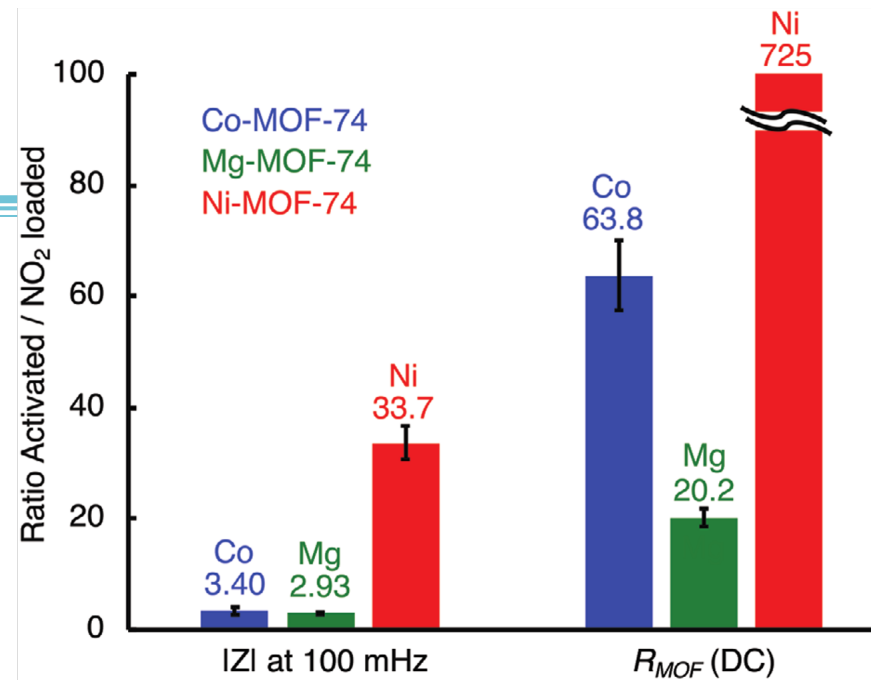
MOF/IDE direct electrical Impedance response of drop cast MOF film (blue) vs. crystallized thin film (red) MOF.

Faster kinetics and response from the thinner thin film version.

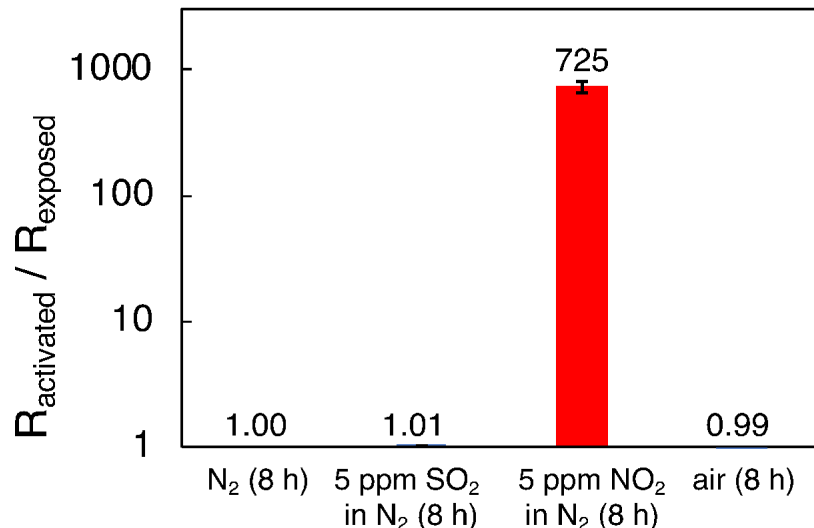


# NO<sub>2</sub> Selective M-MOF based Sensor

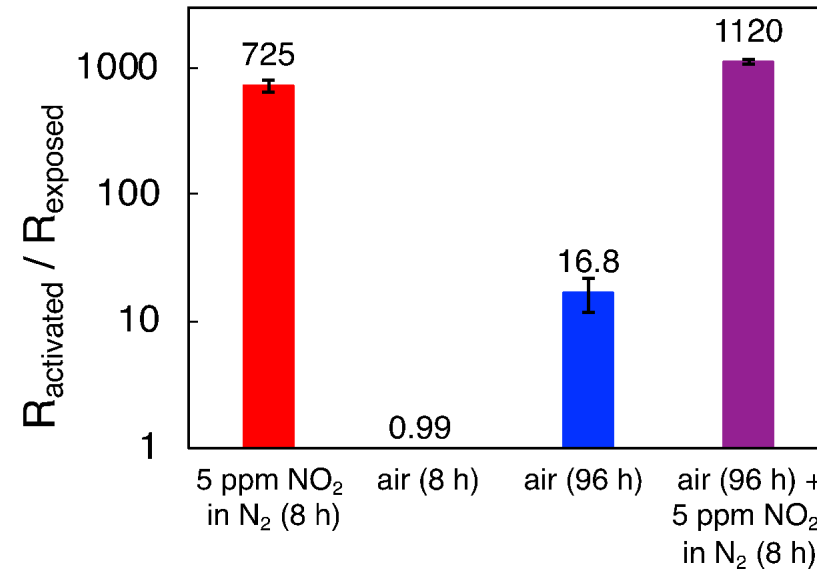
*Small changes in MOF lead to very large electrical response changes in the sensor*



## A. Ni-MOF-74



## B. Ni-MOF-74



Small, L.J.; et.al., *Adv. Func. Mater.* **2020**, *1407*, 2006598.  
 Henkelis, S.E., et.al., *Membranes* **2021**, *11*, 176.  
 Small, L.J. et.al., *I&ECR* **2021**, *60*, *21*, 7998  
 Percival, S.J., et.al., *I&ECR* **2022**, submitted.

## Ratio of response from activated to NO<sub>2</sub>-exposed:

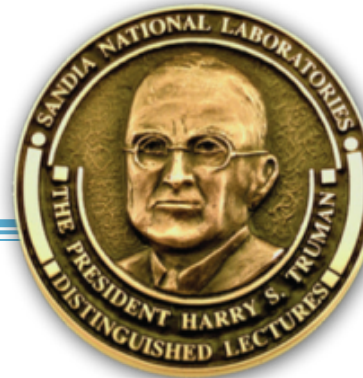
- (1) impedance magnitude at 100 mHz, and
- (2) MOF DC film resistance for IDEs coated with M-MOF-74 (M = Co, Mg, Ni).

NO<sub>2</sub> exposure was at 5 ppm NO<sub>2</sub> for 8h at 50 °C.

## Ratio of Ni-MOF-74 resistance ( $R_{MOF}$ ) when exposed to different environments at 50°C

- highly selective response towards NO<sub>2</sub>.
- (A) 8 h exposures and (B) comparison of response of extended air-exposure combined with subsequent NO<sub>2</sub> exposure.
- “Air” is ambient atmosphere (25 °C 50% RH, 400 ppm CO<sub>2</sub>, 21% O<sub>2</sub>), then heated to 50 °C.

# Sandia Truman Fellowship FY24



## Seeking Applicants!

Sandia National Laboratories is seeking applicants for the **President Harry S. Truman Fellowship** (in National Security Science and Engineering).

Candidates for this position are **expected to have solved a major scientific or engineering problem in their thesis work or have provided a new approach or insight to a major problem**, as evidenced by a recognized impact in their field

The Fellowship provides the opportunity for new Ph.D. scientists and engineers to pursue independent research of their own choosing that supports Sandia's national security mission.

The appointee is expected to foster creativity and to stimulate exploration of forefront S&T and high-risk, potentially high-value research and development.

**Sandia's research focus areas are: bioscience, computing and information science, engineering science, materials science, nanodevices and microsystems, radiation effects and high energy density physics, and geosciences.**

The Truman Fellowship is a **three-year appointment**. The salary is \$111,200 plus benefits and research funding for the proposal.

The deadline is **November 1** of each year and normally begins on October 1 the following year.

## Requirements:

Candidates must meet the following requirements:

- Ph.D. awarded within the past three years at the time of application or completed Ph.D. requirements; with strong academic achievement and evidence of exceptional technical accomplishment, leadership, and ability to team effectively
- Candidates must be seeking their first national laboratory appointment (no previous postdoc at a national laboratory)
- Ability to obtain a DOE "Q" clearance, which requires US citizenship

## Visit

[www.sandia.gov](http://www.sandia.gov)

# Jill Hruby Fellowship FY24



## Seeking Applicants!

Sandia National Laboratories is seeking applicants for the **Jill Hruby Fellowship** in National Security Science and Engineering.

This fellowship aims to develop **women** in the engineering and science fields who are interested in technical leadership careers in national security.

Applicants must display excellent abilities in scientific and/or engineering research and show clear promise of becoming outstanding leaders.

Jill Hruby Fellows have the opportunity to pursue independent research that supports Sandia's purpose: to develop advanced technologies to ensure global peace. **In addition to receiving technical mentorship, Jill Hruby Fellows participate in a unique, prestigious leadership development program.**

Sandia's research focus areas are: bioscience, computing and information science, engineering science, materials science, nanodevices and microsystems, radiation effects and high energy density physics, and geosciences.

The Jill Hruby Fellowship is a **three-year appointment**. The salary is **\$111,200 plus benefits**.

The deadline is **November 1** of each year and normally begins on October 1 the following year.

## Requirements:

Candidates must meet the following requirements:

- Ph.D. awarded within the past three years at the time of application or completed Ph.D. requirements; with strong academic achievement and evidence of exceptional technical accomplishment, leadership, and ability to team effectively
- Candidates must be seeking their first national laboratory appointment (no previous postdoc at a national laboratory)
- Ability to obtain a DOE security clearance, which requires US citizenship

## Visit

**[www.sandia.gov](http://www.sandia.gov)**